ABSTRACT

Title of Document:	ANATOMICAL AND PHYSIOLOGICAL CHARACTERIZATION OF THE TURTLE BRAIN STEM AUDITORY CIRCUIT.
	Katie Leann Willis, Doctor of Philosophy, 2014
Directed By:	Professor Catherine E. Carr, Department of Biology

The goal of this dissertation is to add to understanding of the evolution of hearing by studying the testudine taxon. This dissertation focuses on central auditory processing in the context of evolution. The experiments described are designed to give insight into how binaural hearing evolved.

Follow the findings of Christensen-Dalsgaard and colleagues (2012) that an amphibious turtle had lower hearing thresholds under water than in air and that this difference is conferred by resonance of the middle ear cavity, I examined middle ear cavities across families of Testudines. I found that middle ear cavity structure and function is shared by all testudines (Willis, et al., 2013).

Modern neuroanatomical tract tracing techniques were used to understand the connections among the auditory nuclei in the brain stem of the turtle. Turtles have brain stem nuclei that are connected in the same pattern as the other reptiles, including birds. These nuclei

are nucleus angularis, nucleus magnocellularis, nucleus laminaris, superior olive, and torus semicircularis. Details of neuron structure were also examined and quantified.

Finally, I developed an isolated head preparation that enables in vivo-like physiological recording. As proof of principle, neurons were characterized by best frequency response, threshold, phase locking. Additionally, binaurally responsive neurons were found, which have a range of interaural time difference sensitivity responses.

Although the evolutionary position of testudines is not yet resolved, it is most likely that testudines share their most recent common ancestor with the archosaurs. I hypothesize that testudines likely reflect the ancestral condition of auditory processing for the archosaur clade.

All experiments described in this dissertation were performed according to the guidelines approved by the Marine Biological Laboratory (Woods Hole, MA, USA), the University of Maryland Institutional Animal Care and Use Committees (IACUC) and the Danish National Animal Experimentation Board (Dyreforsøgstilsynet).

ANATOMICAL AND PHYSIOLOGICAL CHARACTERIZATION OF THE TURTLE BRAIN STEM AUDITORY CIRCUIT.

By

Katie Leann Willis

Dissertation submitted to the Faculty of the Graduate School of the
University of Maryland, College Park, in partial fulfillment
of the requirements for the degree of
Doctor of Philosophy
2014

Advisory Committee:
Professor Catherine E. Carr, Chair
Professor Jens Herberholz, Dean's Representative
Professor William Hodos
Professor Arthur Popper
Professor David Yager

Dedication

To Mom and Dad, for everything.

Acknowledgements

I was incredibly fortunate to join Catherine Carr's lab. She has taught me incredible amounts about being a scientist, both directly and by example. Her support and advice has been invaluable. She has given me the support and freedom to be creative in the lab. I am also grateful for the lab environment that she has created that has been so vital to graduate career. The members of the lab, especially Jheeaye Ahn, Caitlin Baxter, Hilary Bierman, Katrina MacLeod, and Sara Therrian, have made daily life in the lab fun and have provided endless scientific support. I particularly acknowledge Angeline Johny, who has been my undergraduate researcher assistant for the past 2 years. She has been invaluable to my projects and the lab. My committee members, Jens Herberholz, William Hodos, Arthur Popper, and David Yager have been invaluable in shaping these projects and have gone above and beyond in their advocacy for my career. I am additionally grateful for the scientific insights of Jakob Christensen-Dalsgaard.

The NACS community has enhanced my graduate school experience. The students and faculty have taught me so much. I am particularly grateful to Susan Teubner-Rhodes and Meghan Riley-Graham for their camaraderie throughout classes and their joy and creativity outside of class. Jeff Chrabaszcz has been a source of statistical knowledge. I am indebted to Alice Jackson for her scientific, baking, and crafting prowess.

Additionally, I am thankful for the support and unconditional love of my family. Outside of academia, I have been kept laughing and thinking by my church family, particularly Elizabeth Kay and Rachel Mumbert. Matt Johnson remained the

voice of calm throughout this process, and I am grateful for his love and his joy. I am grateful for the enduring love and support of my family, especially my parents and my sister.

All experiments described in this dissertation were performed according to the guidelines approved by the Marine Biological Laboratory (Woods Hole, MA, USA), the University of Maryland Institutional Animal Care and Use Committees (IACUC) and the Danish National Animal Experimentation Board (Dyreforsøgstilsynet).

This work was supported by awards from the Danish National Science Foundation 09-065990 and Carlsberg Foundation 2009- 01-0684 (JCD), the Velux Foundation (Denmark), ONR N000140811231 (DRK) and NIH (National Institutes of Health) DC00436 (CEC), and by NIH P30 DC0466 to the University of Maryland Center for Comparative and Evolutionary Biology of Hearing, by training grant DC-00046 from the National Institute of Deafness and Communicative Disorders of the National Institutes of Health and by NSF IIS 9874781 and 0208675 to T. Rowe.

Table of Contents

List of Tables

List of Figures

Chapter 1: Auditory Brain Stem Processing in Reptiles and Amphibians: Roles of Coupled Ears

This chapter is comprised of portions of a previously published work: Willis, K. L., Christensen-Dalsgaard, J., & Carr, C. E. (2013). Auditory Brain Stem Processing in Reptiles and Amphibians: Roles of Coupled Ears. In SpringerHandbook of Auditory Research. New York, NY: Springer New York. doi:10.1007/2506_2013_24

All experiments described in this dissertation were performed according to the guidelines approved by the Marine Biological Laboratory (Woods Hole, MA, USA), the University of Maryland Institutional Animal Care and Use Committees (IACUC) and the Danish National Animal Experimentation Board (Dyreforsøgstilsynet).

1 Introduction

1.1 Overview

Two developments characterize the adaption of the tetrapod auditory system to life in air. These are the development of the tympanum, or eardrum, which allows sensitive responses to airborne sound (Clack, 2002), and the separation of the mouth cavity from the middle ear (Manley, 2010). The ancestors of tetrapods moved onto land in the Devonian, and paleontologists estimate that tympanic hearing emerged about 100 million years later, after the major tetrapod lineages emerged (Clack, 2002)

(Fig. 1.1). Tympanic hearing appears to have developed independently in at least five major tetrapod groups—the anurans (frogs and toads), testudines (turtles and tortoises), lepidosaurs (lizards and snakes), archosaurs (birds and crocodilians), and mammals (Fig. 1.1).

The emergence of a tympanic ear would have increased the frequency range and sensitivity of hearing (Clack, 2002; Christensen-Dalsgaard & Carr, 2008). Further, tympana were in many cases acoustically coupled through the mouth cavity and therefore inherently directional, acting as pressure difference receivers. The later closure of the middle ear cavity, to varying degrees, in turtles and archosaurs is a derived condition, and would have profoundly changed the operation of the ear by decoupling the tympana. This chapter addresses how these changes in the auditory periphery, that is, the evolution of eardrums and coupled ears, could have influenced the organization of the central auditory system. Wilczynski and Capranica (1984) discussed the effect of peripheral changes, and argued that, because new peripheral structures are specializations of preexisting structures, their central systems must also be specializations of (and homologous to) preexisting areas. Thus, a major evolutionary change in the periphery need not initially require a parallel genetic change in brain architecture because the new inputs in the periphery should cause epigenetic rearrangements at other levels of a functional system.

One way to examine the influence of the tympanic ear on the central auditory system is to compare the organization of the auditory system of groups that share a common origin of tympanic hearing. A strongly organizing influence of the tympanic ear would result in homologous neural structures only in groups that share a

homologous tympanic ear. Therefore, anurans, reptiles, and mammals should have central auditory systems that are more similar within each group than among the groups. This idea is supported by the existence of morphotypes, or conserved patterns of organization, observed within each group (Northcutt & Kaas, 1995).

1.2 Basal Patterns Among the Tetrapods

The overall structure of the central auditory system is similar among the vertebrates, and has been reviewed recently (Carr & Edds-Walton, 2008). Similarities between different vertebrate groups cannot be used as evidence for or against an early origin of the auditory system, as opposed to multiple origins, because the similarities could simply reflect the overall organization of the octavo-lateral system (Grothe et al., 2004). With this caveat, in the major vertebrate taxa, the auditory midbrain receives ascending inputs from both monaural and binaural hindbrain nuclei, and physiological recordings have revealed the emergence of complex response properties there (reviews in McCormick, 1999; Grothe, 2003; Carr & Edds-Walton, 2008). The midbrain projects to the thalamus, which in turn projects to auditory stations in the telencephalon. The organization of the telencephalon is structurally and functionally diverse. In all vertebrate clades, the telencephalon exhibits large changes associated with the increased use of sound for communication (Wilczynski & Capranica, 1984). The changes in the auditory periphery outlined above, that is, the evolution of eardrums and coupled ears, may have influenced the organization of the central auditory system in the anurans (frogs and toads), testudines (turtles and tortoises), lepidosaurs (lizards and snakes), and archosaurs (birds and crocodilians). In general,

mammalian middle ears are not coupled, but connected to the mouth via narrow Eustachian tubes.

1.3 Amphibians

Amphibians show great variety in the degree of specialization of the auditory periphery. Most anurans possess a tympanic middle ear sensitive to airborne sound that is processed by the amphibian and basilar papillae (Christensen-Dalsgaard, 2009). Associated with responses to airborne sound, a dorsal medullary auditory nucleus appears in anurans. Its origins and possible homology to the amniote cochlear nuclei are still unclear (Wilczynski & Capranica, 1984). The dorsal medullary nucleus receives tonotopic projections from the amphibian and basilar papillae, as well as inputs from the lagena and possibly the saccule (review in McCormick, 1999). Interestingly, it also receives extensive commissural projections from the contralateral dorsal medullary nucleus, indicating significant binaural interaction at this early stage (reviews in Zakon & Wilczynski, 1988; Christensen-Dalsgaard, 2005).

1.4 Sauropsids or Reptilia

The sauropsids (Reptilia) are a clade that includes testudines (turtles and tortoises), lepidosaurs (snakes and lizards), and archosaurs (crocodilians and birds), as well as a number of extinct groups. The archosaurs are more closely related to each other than they are to the lepidosaurs, while the position of testudines is controversial (Hedges & Poling 1999). Recent molecular phylogenies of testudines support an archosaur affinity (Zardoya & Meyer, 2001; Shen et al., 2011; Crawford et al., 2012). However, other recent analyses support the traditional position of testudines as parareptiles, sister to the entire diapsid (lepidosaurs and archosaurs) clade (Lyson et al., 2010).

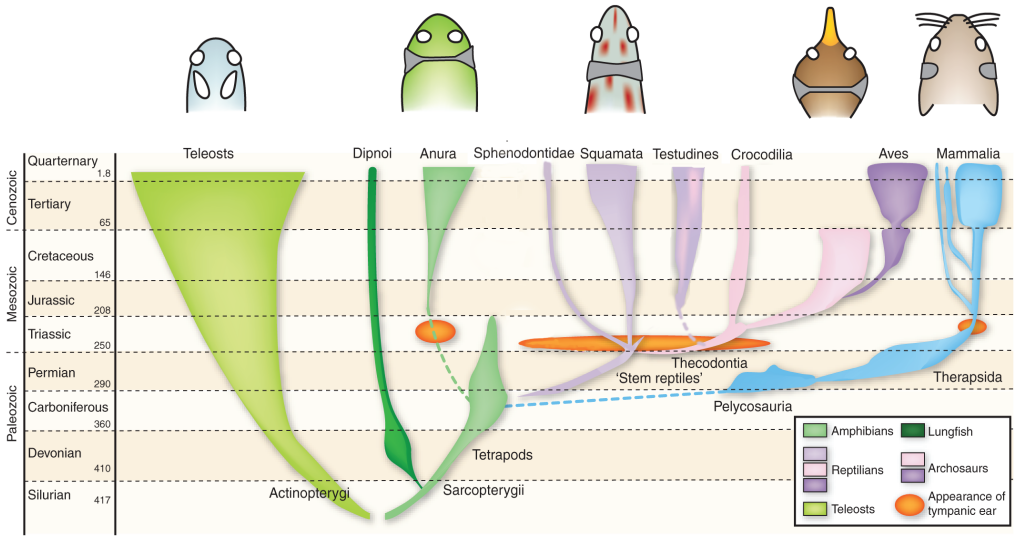

Figure 1.1. Evolution of tympanic ears in vertebrates
The appearances of tympanic ears within the fossil record (orange; Clack & Allin, 2004). These ears exhibit varying degrees of coupling (gray, shown in head schematics on top row) (From Schnupp & Carr, 2009, used with permission)

Despite the great diversity of sauropsids, their central auditory systems show a common plan, suggesting an origin of tympanic hearing before the lepidosaur–archosaur split, especially because the evidence for an independent origin of the tympanic ear in lepidosaurs and archosaurs is weak (Clack & Allin 2004). Most major differences among sauropsid auditory systems are associated with changes in the periphery. The following sections focus on the effects of these changes in the auditory periphery, such as coupled middle ears and the presence of a tympanum.

Reptiles have a tympanum (or tympanic disk), and may or may not have an external ear. In snakes and some lizards, loss of the tympanum is secondary. All have a single middle ear bone, the columella extracolumella, which either connects the tympanum and the oval window, or, in snakes, connects the quadrate and oval window. Movement of the columella activates the hair cells of the basilar papilla (Miller, 1980; Manley, 2000). Sensory hair cells of the basilar papilla are innervated by the auditory nerve, which projects to two nuclei in the dorsal medulla, the nucleus magnocellularis (NM) and the nucleus angularis (NA). NM projects to the second order nucleus laminaris (NL), which in turn projects to the superior olive (SO), to the lemniscal nuclei and to the central nucleus of the auditory midbrain (see Fig. 1.2). Nucleus angularis projects to the superior olive, to the lemniscal nuclei and to the central nucleus of the auditory midbrain. The lemniscal nuclei project to midbrain, thalamic, and forebrain targets. There have been many independent developments superimposed upon this conserved pattern, the details of which have been recently reviewed (Grothe et al., 2004; Carr & Edds-Walton, 2008).

2 Lizards

Lizard ears are highly directional, with middle ears connected through the mouth cavity (Christensen-Dalsgaard & Manley, 2008) (Fig. 1.2). This connection enhances the directionality of the ear by allowing sound access to both sides of each tympanic membrane. The acoustically coupled ears create directional responses from the tympanum (Christensen-Dalsgaard, 2005; Christensen-Dalsgaard & Manley, 2008). Thus, all neurons in the central auditory system should show directional responses, with the possible exception of very low best frequency (below 300 Hz) responses (Christensen-Dalsgaard et al., 2011). In addition, lizards have evolved micromechanical hair cell tuning (Eatock et al., 1981), permitting emergence of sensitive high-frequency hearing in a specialized region of the papilla (Manley, 2002). Thus all lizard auditory responses should be directional, and should include responses to high frequency stimulation.

2.1 Ascending Auditory Pathways

As discussed in Section 1, major differences among central auditory structures appear seldom; these differences are mostly found in the hindbrain and forebrain, with hindbrain changes driven by the development of new end organs in the auditory periphery (Wilczynski & Capranica, 1984). The formation of a new division of the cochlear nucleus angularis (NA) in lizards coincident with the development of a new population of high-frequency hair cells (Szpir et al., 1990) is an example of a central change that appears to result from changes in the periphery.

Lizard inner ears are highly specialized, with sensitive high-frequency hearing originating from a specialized region of the papilla (Manley, 2002). Projections from

the high and low best frequency regions of the papilla form parallel low and high best frequency projections into the nucleus magnocellularis (NM) and the NA (Szpir et al., 1995). Data from tokay geckos (*Gekko gecko*: Tang et al., 2012) and monitor lizards (*Varanus exanthematicus*: Barbas-Henry & Lohman, 1988) show similar patterns of auditory nerve fiber projections, with distinct projections of low and high best frequency fibers to NM and NA. Despite the emergence of these parallel channels, there are otherwise few differences between lizards and other sauropsids in the organization of the auditory brain stem circuits, suggesting homology of the brain stem nuclei (Tang et al., 2012).

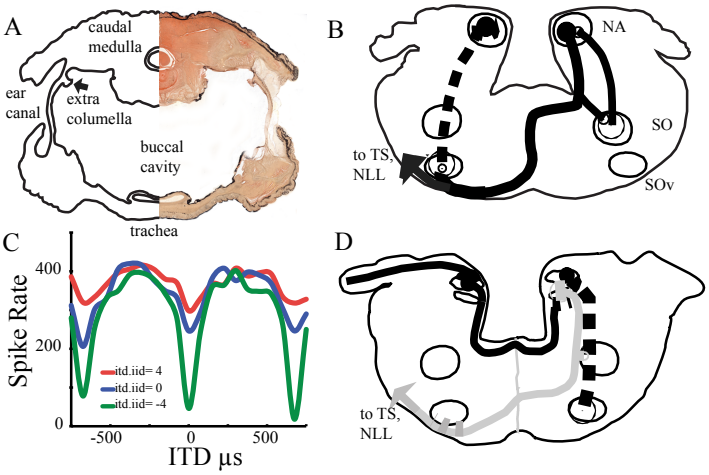

Figure. 2 Pressure difference receiver ear, and connections of the cochlear nuclei and superior olive complex in gecko.

(a) Sound stimulates the tympanum from both the exterior and interior of the head by traveling though the mouth cavity, resulting in a virtually expanded head. View through a Gecko head at the level of the caudal

medulla. This section contains the tympanic membrane, a portion of the extracolumella (arrow), the external ear opening, open middle ear, and the buccal cavity. (From Christensen-Dalsgaard et al., 2011, used with permission.)

(b) NA innervates the ipsilateral superior olive (SO), the contralateral ventral superior olive (SOv), and the contralateral torus semicircularis (TS). The olivary nuclei both project back to the ipsilateral first-order nuclei (dashed lines).

(c) ITD-sensitive recordings from the gecko auditory nerve at 3 interaural level differences (4 and 0 dB). (Data from Christensen-Dalsgaard et al., 2011.)

(d) NM projects to the dorsal neuropil of the ipsilateral NL and across the midline to the ventral neuropil of the contralateral NL, while NL projects to the ipsilateral SO and to the auditory midbrain, through a fiber bundle that descended to run ventral to the contralateral SOv (gray line). SOv projects back to the ipsilateral NM and NL (dashed line). (Data in B, D from Tang et al., 2012.)

2.1.1 First-Order Nuclei and the Nucleus Laminaris

In birds, the auditory nerve tends to form large axosomatic synapses in nucleus magnocellularis, associated with phase locking and the preservation of temporal information, while the projection to nucleus angularis generally forms bouton terminals (Carr & Boudreau, 1991; Ryugo & Parks, 2003). Recent work in tokay geckos showed that auditory nerve terminals in NM form larger boutons than those in NA. This is also the case in the California alligator lizard (*Elgaria multicarinata multicarinata*), where the fibers terminating in medial NM can form axosomatic endings that resemble mammalian and avian endbulbs of Held (Szpir et al., 1990). NM neurons have large ovoid cell bodies, whereas NA contains more heterogenous cell types (Szpir et al., 1995). NM projects bilaterally to NL in geckos (Tang et al., 2012) (Figs. 1.2). Like birds, lizards have an NL, composed of a lamina of bitufted cells that partially overlaps NM (Yan et al., 2010). A clear NL had not been previously observed in other lizard species, but controversy over its presence or absence appears to depend on its correct identification using modern anatomical techniques (Yan et al., 2010). By means of modern techniques, NL is evident in Tokay geckos (*Gekko gecko*) and consists of a distinct population of bitufted calretinin-immunoreactive neurons below the NM. NL receives projections from both ipsilateral and contralateral NM, such that the ipsilateral projection innervates the dorsal NL neuropil, while the contralateral projection crosses the midline and innervates the ventral dendrites of NL neurons.

This connection pattern is similar to that found in birds, in which NL forms a circuit for computing interaural time difference (Young & Rubel, 1983; Carr &

Konishi, 1990; Krützfeldt et al., 2010). Because lizard ears are coupled, all lizard auditory responses should be directional (Christensen-Dalsgaard et al., 2011), begging the question of how NL responds to bilateral inputs. Binaural comparisons are still necessary because monaural directional responses are ambiguous with respect to level and location. Lateralized responses could be generated by rate-based binaural comparisons, similar to the rate-based comparisons in two lateralized channels proposed for the gerbil and guinea pig by McAlpine et al. (2001) and for the cat auditory cortex by Stecker et al. (2005). In the lizard, however, these responses could be generated as early as the lower brain stem. Binaural excitatory–inhibitory comparisons can produce an effective steering toward the sound source (Christensen-Dalsgaard et al., 2011).

In Tokay geckos, NL projects to the contralateral torus semicircularis, and to the contralateral ventral SO (Tang et al., 2012). NL projects to ipsilateral SO, sends a major projection to the contralateral ventral SO, and projects to torus semicircularis (Fig. 1.3). The SO projects to the contralateral ventral SO, which projects back to the ipsilateral NM, NL, and NA. These results suggest homologous patterns of auditory connections in lizards and archosaurs, and also different processing of low- and high-frequency information in the brain stem. The evolution of specialized high best frequency region(s) of the lizard papilla may have driven the development of parallel low- and high-frequency streams in the brain stem. In ancestral atympanate tetrapods, low-frequency sound may have been processed by non-tympanic mechanisms like those in extant amphibians. The subsequent emergence of tympanic hearing would have led to increased sensitivity to higher frequency sounds and potentially to

changes in the central auditory processing in all the tympanate vertebrates. The unitary nature of the auditory experience and the need for adequate auditory steering should, however, have led to mechanisms to link high and low best frequency responses to form single auditory objects by convergence of high- and low-frequency streams in higher stations of the auditory pathway.

2.1.2 Midbrain

The torus semicircularis is the homolog of the inferior colliculus in birds and mammals and is located caudal and ventral to the optic tectum. In lizards, the torus is composed of an auditory central nucleus, surrounded by laminar and superficial nuclei (Díaz et al., 2000). The central nucleus is the recipient of lemniscal fibers and projects to the auditory nucleus of the thalamus (Pritz, 1974; Foster & Hall, 1978; ten Donkelaar et al., 1987). The reported auditory responses in previous studies were probably recorded in the central nucleus (Kennedy, 1974; Kennedy & Browner, 1981; Manley, 1981). The central nucleus is differentiated from the surrounding periventricular regions by distinct patterns of calcium binding protein expression (Yan et al., 2010).

Immunohistochemical studies revealed three subdivisions, a lateral NL and NA recipient subdivision with large calretinin positive fibers and terminals, and a second ventral division delineated by parvalbumin immunoreactive neuropil, which appears to receive input from the olivary and lemniscal nuclei (Yezhong Tang, unpublished observations, 2013). The largest division of the central nucleus is dorsomedial, and it does not appear to receive ascending auditory inputs. It is characterized by calbindin immunoreactivity (Yan et al., 2010).

Tract tracing studies, combined with electrophysiological experiments, are needed to determine whether the gecko torus, like the torus and inferior colliculus in other vertebrates, has divisions based on different afferent inputs (review in Covey & Carr, 2004). The data are consistent with the following hypothesis: there is a restricted lateral distribution of calretinin immunoreactive terminals in the central nucleus that is the recipient zone for input from NA and NL, while a ventral division receives projections from the olivary and lemniscal nuclei. Thus it appears that the central nucleus of the torus is subdivided on the basis of afferent inputs (Yan et al., 2010). This organization resembles the barn owl inferior colliculus, in which input from NL to the central nucleus core abuts an input region of a similar best frequency from the lemniscal nuclei and NA into the central nucleus shell (Takahashi & Konishi, 1988a,b; Wagner et al., 2002). Similar divisions characterize the chicken inferior colliculus (Wang & Karten, 2010).

2.2 Localization and Coupled Ears

Lizards have highly directional ears. The directionality is caused by strong acoustical coupling of the eardrums due to almost unattenuated interaural transmission of sound from the contralateral ear (Christensen-Dalsgaard & Manley, 2005, 2008). The coupled ears in geckos produce directionally sensitive responses in the auditory nerve (Christensen-Dalsgaard et al., 2011) that, in many respects, resemble computed binaural responses from the neural circuits in the avian NL and the mammalian SO nuclei (reviews in Grothe et al., 2010; Ashida & Carr, 2011) (Fig. 1.3). An important difference between gecko auditory nerve and the binaural responses recorded in birds and mammals is that gecko responses reflect the interaction of

ipsilateral and contralateral inputs on the motion of the eardrum and therefore simultaneously encode interaural time and level differences. In free-field stimulation, auditory nerve responses simply reflect the strong directionality of the eardrum (Christensen-Dalsgaard & Carr, 2008). Most or all neurons in the lizard central auditory pathway should be directional. This prediction is supported by results from freefield stimulation of the torus semicircularis of the Tokay gecko (Manley, 1981), in which toral units exhibited directivity with activity almost completely suppressed at ipsilateral angles. The embedded directionality of all auditory responses begs the question of the function and origins of the NM–NL circuit, which resembles the circuit found in other reptiles. The most plausible role for NL is for binaural comparisons. These are still necessary, as any monaural directional response is ambiguous with respect to level and location. Further, the directional response of the eardrum is weaker at low frequencies, so neural processing of low-frequency information by the NM–NL circuit might be important. Eardrum directionality is strongly asymmetric across the midline, so it is possible that lateralized responses could be generated by rate-based binaural comparisons. These would be similar to the rate based comparisons in two lateralized channels proposed for the gerbil and guinea pig (McAlpine et al., 2001) and for the cat auditory cortex (Stecker et al., 2005).

Comparisons between geckos, birds, and mammals may be instructive. In birds and crocodilians, ITD processing is mediated by a circuit in the NL, consistent with the Jeffress model, which assumes arrays of coincidence-detector neurons that respond maximally when phase-locked inputs converge (Jeffress, 1948; Carr &

Konishi, 1990; Overholt et al., 1992; Köppl & Carr, 2008). In mammals, sound source location may instead be computed from the overall discharge rate within the broadly tuned ITD channel on one side of the brain, provided that comparisons with the other ear allow resolution of ambiguity (Lesica et al., 2010). Thus birds use delay lines to map sound location across an array or map of neurons, whereas mammals have no such requirement. The nature of delays in mammals appears multifaceted, whereas in geckos, a fixed acoustic delay across the mouth cancels tympanic motion when it exactly compensates for the ITD presented through earphones or when the delay across the mouth exactly compensates for the sound location in free field. Thus, tokay geckos and lizards should show no range of ITDs in. Instead, there should be broadly tuned ITD channels on each side of the brain.

3 Snakes

Snakes are lepidosaurs that lack both an outer ear and a tympanic middle ear, which in most tetrapods provides impedance matching between the air and the inner ear and hence underlies sensitive hearing of airborne sound. In snakes, and in some earless lizards, the columella instead connects to the quadrate, which should confer acute sensitivity to substrate vibrations (review in Young, 2003). This turns out to be the case; Christensen and colleagues recently showed that detection of cranial vibrations, induced either by airborne sound or by substrate vibration, underlies the inner ear responses of the royal python (*Python regius*: Christensen et al., 2011). Thus, pythons, and possibly all snakes, have lost effective pressure hearing. Their acute vibration sensitivity may instead be used for communication and detection of predators and prey.

Unlike other lepidosaurs, snake ears are not coupled, because snakes do not have tympanic hearing. Nevertheless, effective coupling may occur via the columella's connection to the quadrate. The columellae connect each oval window to the lower jaw, which can rest on the substrate. Prey movements can generate low propagation velocity Rayleigh waves that can vibrate each quadrate (Friedel et al., 2008). Thus, stereo responses to incoming vibrations and sound source localization via coupled quadrates are possible (Friedel et al., 2008).

3.1 Ascending Auditory Pathways

The loss of pressure hearing in snakes might have led to changes in the central circuitry. Miller described two cochlear nuclei, in the pattern of the other sauropsids (Miller, 1980), and used degeneration techniques to show that the auditory branch of the VIIIth nerve projected to NA and NM, whereas NM, in turn, projected bilaterally to NL. Other authors found no NL (Weston, 1936) or only one cochlear nucleus (Holmes, 1903), so modern anatomical analyses of central auditory and vestibular pathways are required to determine which octaval endorgans project to which octaval targets. Are vibration stimuli encoded by NM and NA, or is there cross-talk between central "auditory" and central vestibular targets? Some combination of the first-order nuclei project to torus semicircularis, but there are no detailed studies on this portion of the pathway (Young, 2003). Physiological data from the midbrain show responses to both auditory and vibration stimuli (Hartline & Campbell, 1969; Hartline, 1971a,b). Given the results of Christensen et al. (2011), one assumes that the midbrain auditory responses are derived from vibration stimuli.

4 Turtles and Tortoises (Testudines)

Turtles and tortoises (collectively known as Testudines) are a monophyletic group that occupies a wide range of ecological niches, from the desert to the ocean. With the introduction of molecular techniques to phylogenetics, the traditional position of testudines as the only extant member of parareptilia, as established by morphological studies, has been called into question. Analyses of mitochondrial DNA and nuclear genes suggest testudines are a sister group to the archosaurs (Hedges & Poling, 1999), supported by recent more compete analyses (Shen et al., 2011; Chiari et al., 2012; Crawford et al., 2012).

Testudines hear through stimulation of a cartilaginous tympanic disk, visible through the relatively undifferentiated skin behind the eye. The disk moves via a hinged connection to the bony capsule wall surrounding it (Wever & Vernon, 1956a; Christensen-Dalsgaard et al., 2012). Behind the tympanic disk is the middle ear cavity, which is connected to the mouth by a small Eustachian tube. Laser vibrometry measurements suggest that the air in the middle ear cavity of turtles resonates in the underwater sound field, driving the disk and making the ear more sensitive to sound under water than in air (Christensen-Dalsgaard et al., 2012). This was measured using the auditory brain stem response (ABR, also known as auditory evoked potentials or AEP). Testudines do not have acoustically coupled ears, possibly because they are adapted for underwater hearing (Willis et al., 2013). The turtle auditory papilla is small and, like all amniote papillae, organized tonotopically, such that higher frequency sounds excite the hair cells at the base and lower frequencies those at the apex (Crawford & Fettiplace, 1980).

4.1 Ascending Auditory Pathways

Compared to other members of Reptilia, including archosaurs, little is known about how the central nervous system of testudines processes sound. Some studies have been published, but, like the aforementioned data on snakes, they often conflict and have not been carried out using modern technology.

4.1.1 First-Order Nuclei and the Nucleus Laminaris

Testudines lack a high-frequency region of their papilla (review in Manley, 2010). Their auditory nerve projects to the cochlear nuclei, NM and NA (Marbey & Browner, 1985; Sneary, 1988). NM then likely projects to NL, although there is some question about this (Miller & Kasahara, 1979) because of the difficulty in distinguishing NM from NL. NL appears to grade into the NM at its caudal end, and Glatt suggested that NL developed from NM (1975a,b). This hypothesis is supported by studies in birds that show that NM and NL are derived from partially overlapping rhombomeres (Marin & Puelles, 1995; Cramer et al., 2000). A common origin for NM and NL may also explain the presence of some auditory nerve input to NL (Barbas-Henry & Lohman, 1988; Carr & Soares, 2002). In testudines, NL forms a cluster of neurons beneath NM (Glatt, 1975b; Willis et al., 2011). I hypothesize that the organization of NL in testudines represents the primitive, all low-frequency condition. The reason for describing their NL as primitive is that it does not have a monolayer arrangement of its neurons, although they do have the typical bitufted appearance of NL neurons in archosaurs and lizards (Willis et al., 2011). In the evolutionary line leading to the archosaurs, NL becomes larger and attains a monolayer structure, probably correlated with an extension of NM's and thus also

NL's frequency range. Observations on crocodilians (Glatt, 1975a; Carr & Soares, 2002), as well as birds (Winter & Schwartzkopff, 1961; Köppl & Carr, 1997), show that the caudolateral low-frequency end of the archosaur NL also has no clear monolayer structure, and is closely associated with NM. Testudine NA is fairly round and lies more dorsal and rostral in the brain stem (Miller & Kasahara, 1979). NM runs in a column rostrocaudally and lies ventral and caudal to NA, and consists of densely packed medium to large-sized round cells. NL is smaller and ventral to NM. The cells of NL are loosely distributed (Miller & Kasahara, 1979). The cells of NM, NA and NL react to calcium-binding proteins and cytochrome oxidase (Belekhova et al., 2008). This pattern of immunoreactivity is similar to that in geckos (Yan et al., 2010). Interestingly, NA and NM are larger in pond turtles than in tortoises (Belekhova et al., 2008). This difference should be investigated further, particularly as it pertains to neural processing of sound.

4.1.2 Midbrain

Beyond the hindbrain anatomy, other studies have focused on the midbrain, specifically the torus semicircularis (Belekhova et al., 1985). They also defined an SO with a dorsal and ventral portion, as found in lizards (Ariëns Kappers et al., 1936). Retrograde labeling was used to show that the torus receives input from the contralateral first-order nuclei, the ipsilateral SO, the dorsal and ventral nuclei of the lateral lemniscus, and the contralateral torus. This is the same pattern seen in other reptiles. The torus may project back to the first order nuclei, the ipsilateral SO, the lateral lemniscus, and the contralateral torus semicircularis (Belekhova et al., 1985). Testudines, lizards, birds, and anuran amphibians also all display distinct distribution

patterns of calcium binding protein expression in the torus, with a mostly complementary pattern of calretinin and calbindin in the African clawed frog (*Xenopus laevis*: Morona & González, 2009) and a mostly complementary pattern of calretinin and parvalbumin in turtles (Belekhova et al., 2002). Parvalbumin predominates in a restricted core region of the central nucleus, with calretinin and calbindin in the surrounding peripheral areas of the central nucleus. These complementary patterns of expression in amphibians and reptiles are similar to the patterns of calretinin and acetylcholinesterase expression observed in the core and shell regions of the central nucleus of the barn owl inferior colliculus (Takahashi & Konishi, 1988b; Adolphs, 1993). In turtles, midbrain there is also a core-and-belt organization: a core that is a "relay" and a belt that has both auditory and somatic inputs (Belekhova et al., 2008, 2010 and Section 3).

Testudine torus neurons of the central nucleus are mostly small to medium in size and vary in shape (Belekohova et al., 2010). They have reciprocal connections with the contralateral intercollicular nucleus. The core and belt regions generally have different chemical characteristics and receive inputs from and send projections to different targets (Belekhova et al., 2010). The central nucleus projects bilaterally to the nucleus reuniens of the dorsal thalamus (Belekhova et al., 1985). These data suggest that the turtle auditory mesencephalon is very similar to that of birds and crocodiles. In order to determine whether or not these areas are homologous, as suggested by Belekhova et al. (2010), developmental, molecular, and genetic studies will be required.

4.2 Localization and Specialization

As amphibious animals, many turtle species face the problem of hearing both in air and underwater. Because of different density and sound velocity in the two media, an ear's impedance-matching mechanisms would be different, and trade-offs are made regarding sensitivity to in-air versus underwater sound (Hetherington, 2008). Further, testudines largely respond to low-frequency sounds, as shown by audiograms (Wever & Vernon, 1956b,c; Patterson, 1966; Ridgway et al., 1969; Bartol et al., 1999). Combined with generally small head widths, this could result in difficulty in localizing sound. Using laser vibrometry and auditory brain stem responses, Christensen-Dalsgaard and co-workers (2012) investigated the auditory sensitivity of the red-eared slider, an amphibious pond slider (*Trachemys scripta elegans*), using both sound and vibration stimuli. The laser vibrometry showed peak vibrations at 500–600 Hz (maximal transfer function of 300 μm/s/Pa). The auditory evoked potential audiogram from the same study was V-shaped with a best sensitivity to airborne sound of about 300–500 Hz. Underwater, the ear was about 10 dB less sensitive to sound; in terms of sound pressure level (SPL), however, the hearing thresholds underwater were about 20–30 dB lower than thresholds in air. One possible explanation for turtles' increased sensitivity to sound under water is that the large middle ear cavity resonates in the underwater sound field. Examining the anatomy of the middle ear cavity and associated auditory structures, Christensen-Dalsgaard et al. (2012) found that the compliant tympanic disk was the critical sound-receiving structure, and attached to a columella/extracolumella that ran through the middle ear cavity.

The organization of the turtle ear resembles that of the aquatic African clawed frog in that both have an air space in the middle ear that can resonate in the underwater sound field, driving a cartilaginous tympanic disk (Fig 2.1; Christensen-Dalsgaard et al., 2012; Willis et al, 2013). This similarity suggests similar selection pressures on the development of an effective aquatic ear. The proposed model for middle ear function in turtles and aquatic frogs resembles other examples of air-filled swim bladders coupled to the ear or lateral line system (Webb et al., 2008). In otophysine fishes, for example, this complex can increase sound sensitivity by 40 dB or more (Popper & Fay, 2011).

A recent study examining the morphology and allometry of middle ear cavities across extant and extinct species supports this hypothesis (Willis et al., 2013). This study demonstrated that allometry and morphology are unchanged across testudines. Further, regardless of phylogenetic position or ecological niche, the middle ear cavity has a volume and morphology that improves hearing thresholds under water by resonance. These data lend further support to an aquatic origin for testudines (Willis et al., 2013) and also raise the question of how testudines localize sound. Their low-frequency hearing, combined with relatively small heads and uncoupled ears, should make sound localization by detection of interaural time differences difficult.

5 Crocodilians

Crocodilians share an archosaur common ancestor with the birds, and the central auditory pathways of the two groups are very similar, although the hearing range of crocodilians is lower (up to 2.9 kHz for Caiman) (Manley, 1970a; Higgs et

al., 2002). Like birds, crocodilian middle ears are coupled via sinuses (Witmer & Ridgely, 2009; Bierman et al., 2011). The inner ear is large, with a long basilar membrane and unidirectional population of hair cells covered by a tectorial membrane (Düring et al., 1974; Wever, 1978). Auditory nerve units are relatively sharply tuned, and phase-lock to frequencies up to 1.5 kHz (Manley, 1970a; Smolders & Klinke, 1986).

5.1 Ascending Auditory Pathways

The auditory nerve projects to NA and NM (Leake, 1974). NA lies anterior to the root of the auditory nerve and is composed of large and small ovoid cells, whereas NM contains characteristic large round principal cells and is larger than NA (Leake, 1974). NM has lateral and medial divisions, with the caudal part of the medial division capped by a small-celled component (Glatt, 1975a,b). There is a similar small-celled region of NM of the bird that receives low best frequency auditory nerve fibers (Köppl, 1994; Köppl & Carr, 1997).

Crocodilian cochlear nuclei are tonotopically organized in a similar fashion to birds (Konishi, 1970; Manley, 1970b). Recordings from the cochlear nucleus in the caiman produced primary-like responses that were very similar to those in the some lizards and all birds (Manley, 1970a, 1974), except that, curiously, one of the tonotopic axes is reversed compared to birds. The crocodilians have a well developed NL, which forms a sheet of bipolar spindle-shaped cells that is very similar to that seen in the basal land birds (Carr, 1993) (Fig. 5a, b). NA and NL project bilaterally to the torus, as is also the case in other sauropsids.

5.2 Localization

Crocodilians are successful predators that hunt on both land and in water. Experimental behavioral evidence of sound localization is lacking, but most crocodilians are nocturnal hunters, and can produce a loud roaring call (Todd, 2007). Further, females can localize the contact calls made by their young (Hunt & Watanabe, 1982; Passek & Gillingham, 1999), so I hypothesize that sound source localization is behaviorally relevant to this group.

Crocodilians have well-developed neural circuits for encoding ITD (Carr et al., 2009). Both avian and crocodilian auditory circuits appear to conform to the requirements of the Jeffress model (Jeffress, 1947; Joris et al., 1998; Ashida & Carr, 2011) (Fig. 1.3). The auditory nerve and NM phase-lock to sound in birds and crocodilians (Köppl, 1997), while NM target neurons in NL act as coincidence detectors for both tones and noise. Internal delays, equal and opposite to interaural delays, characterize barn owls (Carr & Konishi, 1990; Peña et al., 2001), chickens (Overholt et al., 1992; Funabiki et al., 1998; Köppl and Carr, 2008), and alligators (Carr et al., 2009). Best delays in alligator NL are such that neurons respond maximally to sound sources in the contralateral hemifield. Similarly, response delays to contralateral clicks are longer than to ipsilateral clicks (Wagner, 2005; Köppl & Carr, 2008). Thus the axonal delays from NM appear sufficient to account for the range of observed ITDs in alligators.

An additional feature of the Jeffress model is a systematic representation of ITDs, creating a place code of azimuthal position. There is support for a place code in the barn owl in vivo (Carr & Konishi, 1990) and in the chicken, both in vitro

(Overholt et al., 1992) and in vivo (Köppl & Carr, 2008). Data from alligators also support a place code, in that the distribution of lesions made at a range of best ITDs exhibits a trend from medially located best ITDs near 0 to laterally located best ITDs in the contralateral hemifield. The range of best ITDs was very large, however, with median values of about 450 μs, as compared to about 90 μs in chickens (Köppl & Carr, 2008) and 173 μs in the gerbil (Pecka et al., 2008). These are consistent with increased interaural delays from ears coupled by sinuses (Calford & Piddington, 1988; Bierman et al., 2011).

6 Birds

Birds are a sister group to the crocodilians, and their central auditory pathways are very similar. These similarities may be general archosaur synapomorphies (Clack, 1997, 2002), allowing us to hypothesize that similar pathways characterized the auditory systems of the extinct dinosaurs (Witmer & Ridgely, 2009). Dinosaurs may have been both vocal and sensitive to low-frequency sound, since CT scans of the braincase region of tyrannosaurs show that the cochlea is short (Witmer & Ridgely, 2009). Analyses in living archosaurs of best audiogram frequency versus body mass also suggest that in the larger dinosaurs hearing may have been restricted to low frequencies (below 3 kHz) (Gleich et al., 2005).

For birds, the connections and physiology of the auditory system and avian communication have been recently reviewed (Grothe et al., 2004; Moss & Carr, 2012) and this chapter only summarizes them. This chapter focuses on evidence for the role of coupled ears (Köppl, 2009) (Fig. 1.3). Archosaurs have sinuses or cranial air spaces that connect their ears. CT scans of the braincase region of tyrannosaurs

and other dinosaurs (theropoda and ankylosauria) reveal the presence of extensive air filled spaces (Witmer & Ridgely, 2009). These sinuses are well developed in birds, which have pneumatized skulls. In particular, the rostral tympanic recess is large, with a broad contralateral communication ventral to the brain cavity. This connection is also termed the interaural canal, because it connects the two middle ears (Hill et al., 1980; Coles & Guppy, 1988). This coupling is far weaker in birds than lizards (Klump, 2000), but appears effective at low frequencies, where it leads to larger interaural time and level differences than would be predicted from head size (Calford & Piddington, 1988; Köppl, 2009; Christensen-Dalsgaard, 2011).

6.1 Ascending Auditory Pathways

In birds, as in other reptiles, the auditory nerve projects to the NA and NM (Carr & Boudreau, 1991) (Fig. 1.3). NM projects bilaterally to NL (Young & Rubel, 1983), which in turn projects to the SO and the inferior colliculus (Takahashi & Konishi, 1988b). NL computes the time difference between the two ears, while NA receives sound intensity information from the auditory nerve and projects directly to the SO, the dorsal nucleus of the lateral lemniscus and the inferior colliculus (Takahashi & Konishi, 1988b; Euston & Takahashi, 2002). The superior olive provides γ-aminobutyric acid (GABAergic) feedback projections to NA, NM, and NL (Carr et al., 1989; Burger & Rubel, 2008; Wild et al., 2010).

In owls NM is the origin of a neural pathway that encodes timing information, while a parallel pathway for encoding sound level originates with NA (Takahashi, 1989). Recordings in the chicken cochlear nuclei have found a similar but less clear segregation of function. The similarities between owls and chickens suggest that the

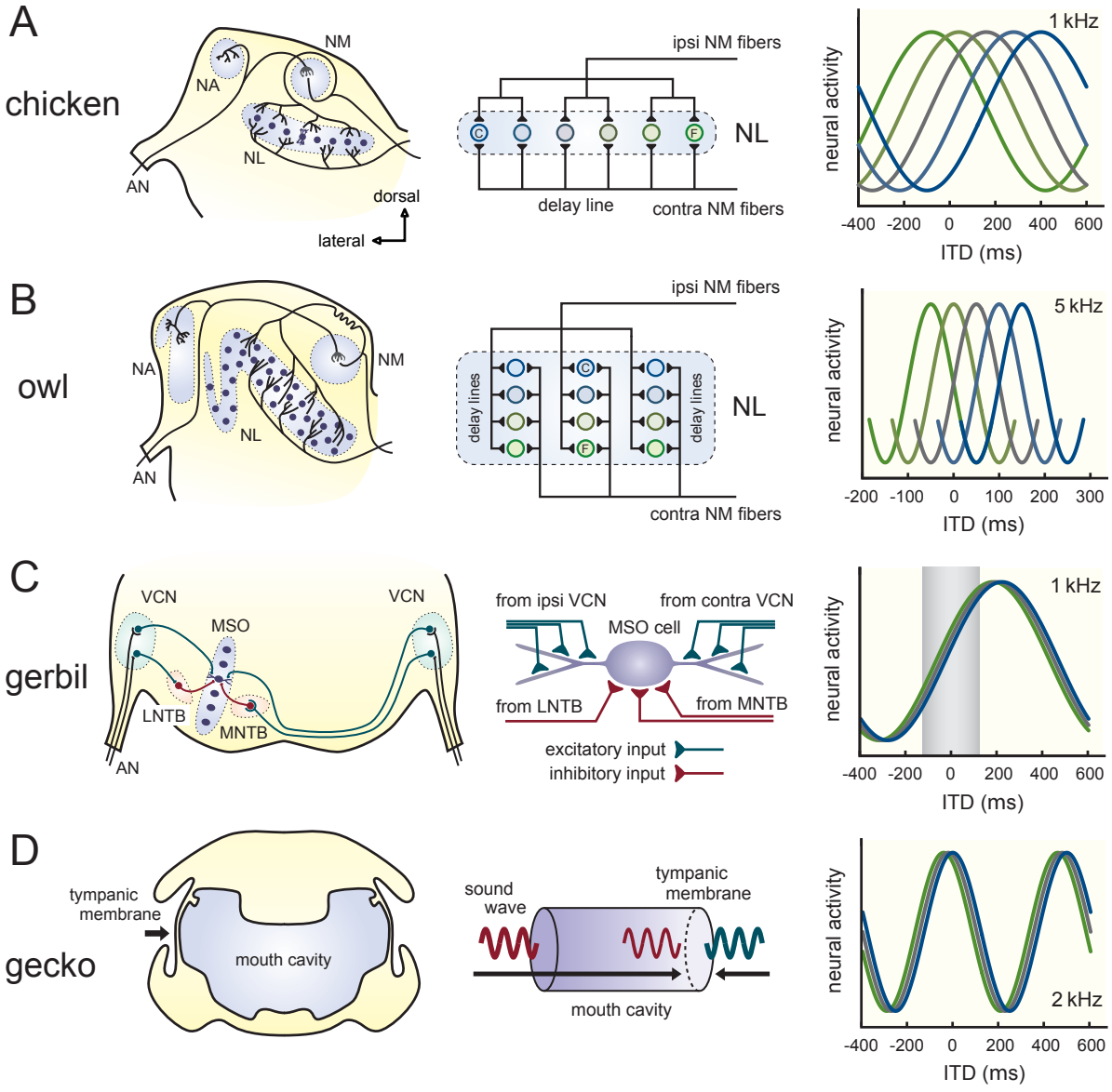
A
chicken
NM
NA
NL
AN
dorsal
lateral
ipsi NM fibers
C
F
NL
delay line
contra NM fibers
1 kHz
neural activity
-400 -200 0 200 400 600
ITD (ms)
B
owl
NA
NM
NL
AN
ipsi NM fibers
delay lines
C
F
delay lines
NL
contra NM fibers
5 kHz
neural activity
-200 -100 0 100 200 300
ITD (ms)
C
gerbil
VCN
VCN
MSO
LNTB
MNTB
AN
from ipsi VCN
from contra VCN
MSO cell
from LNTB
from MNTB
excitatory input
inhibitory input
1 kHz
neural activity
-400 -200 0 200 400 600
ITD (ms)
D
gecko
tympanic membrane
mouth cavity
sound wave
tympanic membrane
mouth cavity
2 kHz
neural activity
-400 -200 0 200 400 600
ITD (ms)

Fig. 1.3 ITD circuit and coding strategies across taxa.
(a) Chicken's ITD coding circuit. (Left) Schematic drawing of the chicken's brain stem. Axons from the ipsilateral NM enter NL dorsally, while those from contralateral NM enter ventrally. NL neurons are aligned in a thin flat layer. (Center) Jeffress-type organization of the chicken's NM NL circuit. Axonal conduction times lead to a place map in NL. Neurons near the lateral border of NL (marked as C) response maximally to sounds coming from the far contralateral side, and cells located close to the medial edges of NL (marked as F) fires maximally to sounds originating from in front of the animal's head. (Right) Example ITD-response curves of NL cells tuned at 1 kHz. As stated previously, the peak position of the tuning curve depends on the location of the neuron in the place map. Positive ITD values mean contralateral ear leading (i.e., sound arrives earlier at the contralateral ear than at the ipsilateral ear). (b) Owl's ITD coding circuit. (Left) Schematic drawing of the owl's brain stem. Similar to the chicken brainstem, axons from the ipsilateral NM enter NL dorsally, while those from contralateral NM enter ventrally. Owl NL neurons, however, are not aligned in a layered structure, but are distributed sparsely throughout the nucleus. (Center). Multiple Jeffress-type place maps of the owl's NM-NL circuit. Gradual changes in axonal conduction times along the dorsoventral dimension result in multiple place maps of NL cells. Neurons near the dorsal border of NL (marked as C) response maximally to sounds coming from the far contralateral side, and cells located close to the ventral edges of NL (marked as F) fires maximally to sounds originating from in front of the animal's head. (Right) Example ITD-response curves of NL cells tuned at 5 kHz. As in chickens' place map, the peak position of the tuning curve depends on the location of the neuron in the place map. (c) Gerbil's ITD coding circuit. (Left) Schematic drawing of the Fig. 5 (continued) gerbil's brainstem. Spherical bushy cells in the VCN provide excitatory inputs to the MSO, while LNTB and MNTB neurons, which receive outputs of the globular bushy cells in the ipsi- and contralateral VCN, respectively, send glycinergic inhibitory inputs to MSO. (Center). Schematic picture of a gerbil MSO neuron. The principal neuron of the MSO has bipolar dendrites segregating ipsi- and contralateral excitatory inputs from the VCN. Inhibitory inputs from LNTB and MNTB are confined to the cell body region. (Right) Example ITD-response curves of MSO cells tuned at 1 kHz. In contrast to chicken's NL cells, the tuning curves of MSO neurons are very similar. Peak positions of the tuning curves can lie out of the physiological ITD range (i.e., ITDs encountered naturally) shown by the shaded area. (d) Gecko's ITD coding. (Left) Schematic drawing of the gecko's head. The inner ears of the gecko are interconnected through the mouth cavity. (Center) Gecko's ear as a pressure gradient receiver. Sound wave arriving at one ear travels through the mouth cavity to reach the tympanic membrane (eardrum) of the other ear, resulting in binaural sound interactions. The motion amplitude of the eardrum changes with the phase difference between the two sounds from inside and outside the ear. (Right) Example ITD-response curves of auditory nerves tuned at 2 kHz. ITD-dependent changes in the motion amplitude of the tympanic membrane results in the spike rate modulation of the auditory nerve in an ITD-dependent manner. Note that the trough of the ITD-response curve at around 200–250 ms corresponds to the conduction delay of sound through the mouth cavity. AN, auditory nerve; NA, nucleus angularis; NM, nucleus magnocellularis; NL, nucleus laminaris; VCN, ventral cochlear nucleus; LNTB, lateral nucleus of the trapezoid body; MNTB, medial nucleus of the trapezoid body; MSO, medial superior olive. (From Ashida & Carr, 2011, used with permission.)

functional separation of time and level coding may be an emerging feature of the avian auditory system. Separation of time and intensity information should not characterize animals with strongly coupled ears, however, or characterize low best frequency processing in birds, as ITD and ILD co-vary when ears are coupled.

The pathway for coding sound level begins with the cochlear NA, which responds to changing sound level over about a 30-dB range (review in Carr & Code, 2000). Each NA projects to contralateral dorsal nucleus of the lateral lemniscus (Krützfeldt et al., 2010; Wild et al., 2010). In barn owls, processing of level differences between the two ears begins in the lemniscal nuclei (review in Carr & Code, 2000). These level differences are produced by the shadowing effect of the head when a sound source originates from off the midline (Klump, 2000), and at low frequencies are intensified by coupling through the interaural canal (Larsen et al., 2006). Neurons of the dorsal nucleus of the lateral lemniscus do not encode elevation unambiguously, and may be described as sensitive to interaural level difference, but not selective because they are not immune to changes in sound level. The encoding of elevation improves in the auditory midbrain (reviews in Tollin, 2008; Grothe et al., 2005).

6.2 Localization

The coupling between the two ears is most effective at low frequencies (Hill et al., 1980; Coles & Guppy, 1988; Hyson, 2005; Köppl, 2009). Physiological recordings in brain stem and cochlear microphonics reveal much larger interaural time differences for low frequency sound stimulation than would be predicted from head size. For sounds above about 2–3 kHz, however, the interaural pathway acts as an acoustical low-pass filter, and sound is attenuated too much for a pressure gradient

mechanism to be effective (Moiseff & Konishi, 1981; Calford & Piddington, 1988; reviews in Klump, 2000; Christensen-Dalsgaard, 2011). Cochlea microphonic and neurophysiological recordings from a number of birds reveal interaural delays at high frequencies that are close to those expected from path length around the head, while delays measured at low frequencies are more than three times this expectation (Calford & Piddington, 1988; Köppl, 2009)

7 Summary and Conclusions

A great deal of the variation in tetrapod auditory systems is peripheral (Wilczynski & Capranica, 1984). Indeed, the tetrapod tympanic ear is a homoplaseous novelty, which has been modified and adapted to various lifestyles over the course of evolution (Manley & Köppl, 1998). In contrast, central processing may be largely conserved. The nuclei not only appear to be homologous (Tang et al., 2012), but also retain similar functions in the different groups. The changes in the central nervous system caused by the emergence of the tympanic ear may include the addition of high-frequency responses in existing nuclei and a requirement for additional binaural processing in those groups that have developed uncoupled or partially uncoupled ears, such as turtles and birds. There are otherwise few differences in the organization of the auditory brain stem circuits of all the groups discussed.

Chapter 2: Middle Ear Cavity Morphology is Consistent with an Aquatic Origin for Testudines

This chapter is comprised of previously published work: Willis, K. L., Christensen-Dalsgaard, J., Ketten, D. R., & Carr, C. E. (2013). Middle ear cavity morphology is consistent with an aquatic origin for testudines. (A. Iwaniuk, Ed.) Public Library of Science ONE, 8(1), e54086.

1 Introduction

Vocalizations indicate that hearing has behavioral importance for Testudines (Carr, 1969). Sea turtles vocalize in air with ‘‘ [a] mercy cry and roars and grunts of anger’’ (Campbell & Evans, 1972). Many species of testudine vocalize in air, most often in the context of mating or distress, including Desert tortoises (*Gopherus agassizzi*), Red-footed tortoises (*Geochelone carbonaria*), Travancore tortoises (*Geochelone travancorica*), Aladabra giant tortoises (*Geochelone gigantean*), and Big-headed turtles (*Platysternon megacephalum*) (Campbell & Evans, 1967; 1972; Frazier & Peters, 1981). Calls of *G. agassizzi* range from 500 to 1000 Hz (Campbell & Evans, 1967). Campbell and Evans characterized one of these calls as a possible distress signal because this particular animal was attempting to escape (Campbell & Evans, 1967). In one recorded instance, the male of a pair of *G. carbonaria*, vocalized in air while he attempted to mount the female. The vocalization is a ‘‘cluck’’ that is paired with head-bobbing behavior. The authors speculate that it is similar to the attraction calls observed in other species, which are used both in mating and in

parent-offspring interactions (Campbell & Evans, 1967; A. F. Carr, 1969). Campbell and Evans further characterize the vocalization of *G. carbonaria* (Campbell & Evans, 1967).The cluck previously described was in the range of 500–2500 Hz. Playbacks of ‘‘cluck’’ recordings elicit head movements. *G. travancorica* is, thus far, the only tortoise species that is known to call in chorus (Campbell & Evans, 1972). These vocalizations had the most energy from 1700–2000 Hz. *P. megacephalum* produces a two-part call with frequency components from 500–4000 Hz. Campbell and Evans observed this particular type of vocalization only in juveniles. Aside from these studies, little to nothing is known about the behavioral and social relevance of any testudine vocalizations.

The best candidate species for investigations of the behavioral relevance of vocalization among the Testudines is *Chelodina oblonga* (Oblong Turtle or Snake-necked Turtle), which exhibits an extensive vocal repertoire that can be divided into 17 categories, including both percussive and complex vocalizations (Giles et al., 2009). Animals of different ages and both sexes were recorded vocalizing in air and underwater. These vocalizations range in frequency from 100 Hz to over 20,000 Hz, a much greater range than is found on other previously studied species. Despite this wide range, the calls are almost all under 4 kHz. The frequency spectra are also quite varied, from harmonic to noisy. This species inhabits turbid water, thus decreasing its ability to use visual cues (Giles et al., 2009). This suggests a reliance on non-visual cues. The spectra covered by these calls do not necessarily imply that the animal can hear the calls throughout the entire range. Birds do not hear the entire spectra of their

song; some of the spectra is higher harmonics as a result of the structure of the vocal apparatus (Konishi, 1970).

Neither the anatomical structures involved in vocalization nor their hearing thresholds have yet been described for *C. Oblonga*. Given this evidence for middle- and high-frequency vocalizations, it is possible that some pleurodires (side-necked turtles), including *C. oblonga*, may hear above 2 kHz, i.e. above reported hearing thresholds (Giles et al., 2009). Taking new findings about vocalizations into account, the idea that turtles are relatively insensitive to sound should be reconsidered. If vocalizations are important for mating or other social interactions, there would be selective pressure for auditory acuity. Given that multiple species vocalize, some at frequencies higher than previously measured, hearing in these species should be more fully investigated.

Testudines are divided into two suborders: Cryptodira and Pleurodira. Extant cryptodires include three superfamilies: Chelonioidea, Testudinoidea, and Trionychoidea. Pleurodires, (Sidenecked Turtles) include the superfamily Pelomedusoidea and the family Chelidae. Testudines, while monophyletic, have adapted to a wide variety of ecological niches and lifestyles (Guillon et al., 2012). Ecologies range from marine (Sea Turtles) to semi-arid desert biomes (Tortoises). Sound transmission, production, and reception are affected by the medium in which the animal lives and communicates. Environmental sounds, as well as those generated by predators, prey, and conspecifics provide essential information.

Multiple skull bones comprise the middle ear cavity (Gaffney, 1972). As in other tetrapods, the inner ear is encased by the cavum labyrinthicum. The interior of

the middle ear cavity is called the cavum tympani, which is formed from the quadrate and the squamosal. The middle ear is bordered anterolaterally and dorsally by the quadrate, dorsally by the opisthotic, medially by the prootic and opisthotic, and ventrally by pterygoid. The columella extends from the oval window, where it forms the stapedial footplate (Wever, 1978), through the cavum acustico-jugulare and incisura columellae auris, into the middle ear cavity. The columella is the primary transducer of sound as demonstrated by Wever and Vernon who showed that the hearing capability of an animal was greatly reduced after the columella was clipped (Wever & Vernon, 1956). The columella terminates on the extracolumella via a short, hinged joint (Christensen-Dalsgaard et al., 2012; Wever & Vernon, 1956). The extracolumella is cartilaginous and forms the tympanic disk.

In *Trachemys scripta elegans* (Red-eared Slider turtle), the tympanic disk is about 0.5 mm thick (Christensen-Dalsgaard et al., 2012; Wever & Vernon, 1956). The tympanic disk is visible on the animal through the relatively undifferentiated skin (Fig. 1), which adheres to the tympanic disk by a thin layer of connective tissue (Christensen-Dalsgaard et al., 2012; Wever, 1978). The tympanic disk moves via a hinged connection to the bony capsule wall surrounding it (Christensen-Dalsgaard et al., 2012; Wever & Vernon, 1956). The disk is primary sound receiving structure of the turtle ear (Adrian, Craik, & Sturdy, 1938; Christensen-Dalsgaard et al., 2012; Wever, 1978; Wever & Vernon, 1956) (Fig. 1). Behind the tympanic disk is the middle ear cavity. Laser vibrometry measurements suggest that the air in the middle ear cavity resonates in the underwater sound field, driving the tympanic disk (Christensen-Dalsgaard et al., 2012).

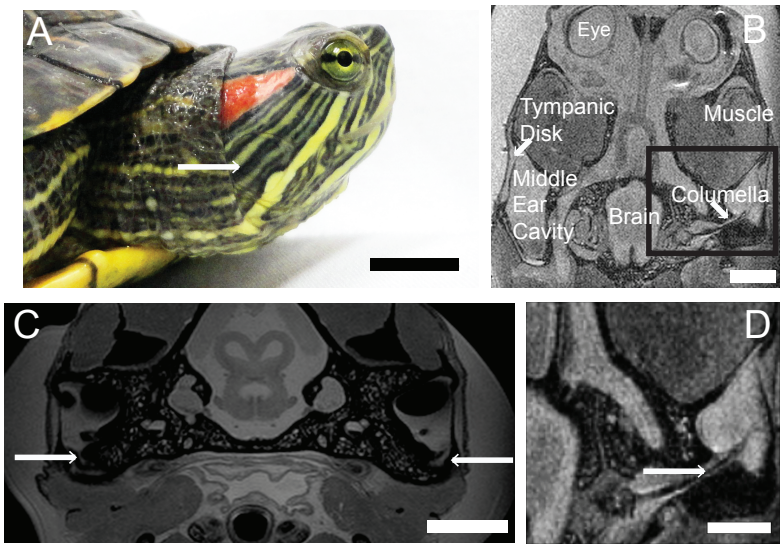

Figure 2.1. Anatomical structures of the testudine auditory system in *Trachemys scripta elegans*.
A. Lateral view of head (1 cm scale bar).
B: Horizontal MR image. (500 mm scale bar)
C: Transverse MRI at the level of the tectum. Arrows indicates Eustachian tubes (500 mm scale bar). ‘‘Muscle’’ is the splenius capitus.
D: Horizontal MR image, enlarged from box in B. The columella runs through the middle ear cavity to the inner ear. Arrow indicates the columella (500 mm scale bar).

Comparisons of hearing in air and under water in *Trachemys scripta elegans* show these turtles are more sensitive to sound under water (Christensen-Dalsgaard et al., 2012). These findings raise many questions. Greater sensitivity to sound under water could be conferred by multiple adaptations. Christensen-Dalsgaard and colleagues suggest that the origin of greater sensitivity to underwater sound is the ability of the middle ear cavity to resonate in the underwater sound field, increasing sensitivity at resonant frequencies (Christensen-Dalsgaard et al., 2012). Is this type of middle ear cavity is a feature of all turtles and tortoises, or is it only found in those testudines that spend significant time underwater? How do variations in middle ear structures inform our understanding of the evolutionary history of testudines? We demonstrate here that middle ear scaling and morphology is similar across extant species, regardless of ecological niche or phylogenetic position.

2 Methods

2.1 Imaging

We examined the middle ear cavity and associated structures using X-ray computed tomography (CT) and magnetic resonance imaging (MRI) (Table 2.1). Specimens (*Trachemys scripta elegans* and *Macroclemys temminckii)* were prepared for magnetic resonance (MR) scanning by euthanasia via an overdose of Euthasol (Virbic Animal Health, Fort Worth, TX). The heads were then removed and immersion-fixed in 4% paraformaldehyde (PFA) in 0.01 M phosphate buffered saline (PBS) for a minimum of 1 week. The fixed heads were rehydrated in 0.01 M PBS a minimum of 24 hours before the scan. In order to optimize the image the middle ear cavities were filled with PBS: one syringe was inserted into the tympanic disk to

Suborder	Superfamily	Family	Subfamily	Species	Ecology
Pleurodira		Chelidae		*Elseya dentata*	Aquatic
				Chelus fimbriatus	Aquatic
	Pelomedusoidea	Podocnemididae		*Pelusios sinuatus*	Aquatic
				Podocnemis unifilis	Aquatic
Cryptodira	Trionychidea	Carettochelyidae		*Carettochelys insculpta*	Aquatic
		Dermochelyidae		*Dermochelys coriacea*	Marine
		Kinosternidae	Staurotypinae	*Staurotypus salvinii*	Aquatic
			Kinosterninae	*Kinosternon bauri*	Aquatic
		Trionychidae	Trionychinae	*Trionyx triunguis*	Aquatic
				Apalone mutica	Aquatic
	Testudinoidea	Platysternidae		*Platysternon megacephalum*	Dual
		Bataguridae	Geoemydinae	*Rhinoclemmys pulcherrima*	Terrestrial
				Cuora amboinensis	Dual
		Emydidae	Emydinae	*Glyptemys (Clemmys) muhlenbergii*	Dual
				Emys orbicularia	Aquatic
				Malaclemys terrapin	Aquatic
			Deirochelyinae	*Trachemys (Pseudemys) scripta elegans*	Aquatic
				Chrysemys picta picta	Aquatic
		Testudinidae (Tortoises)		*Testudo horsfieldi*	Terrestrial
				Gopherus polyphemus	Terrestrial
		Chelydridae		*Chelydra serpentina*	Aquatic
				Macroclemys temminckii	Aquatic
	Chelonioidea (Sea Turtles)	Cheloniidae		*Carretta caretta*	Marine
				Chelonia mydas	Marine
				Lepidochelys kempii	Marine

Table 2.1: Phylogenetic relationships of the species studied. At least one representative from each family of testudines was included in this study, with the exception of the Dermatemydidae, a monotypic family containing *Dermatemys mawii* for which no museum specimen was available.

remove air while another syringe was simultaneously used to inject 0.01 M PBS. Trachemys scripta elegans was chosen as an example species for an allometric series because it is an amphibious invasive species and commercially available. Animals were obtained from a commercial dealer. Furthermore, the small head size allowed imaging in the most powerful MR scanner (9.4 T). MR images of M. temminckii and T. scripta elegans were acquired at the Armed Forces Institute of Pathology (Rockville, MD). Prior to imaging, larger heads were sealed in a plastic bag filled with 0.01 M PBS and imaged with a 72 mm volume coil on a Bruker Biospec spectrometer (Bruker Biospin, Inc. Billerica, MA) coupled to a horizontal-bore magnet (diameter: 20 cm) operating at 7 T (300 MHz for protons) using a Rapid Acquisition with Relaxation Enhancement (RARE) sequence with the following acquisition parameters: TR/TE =1500/10 ms, NA=4, RARE= 8. Small heads were immobilized in glass tubes (o.d. 25 mm) filled with PBS and imaged with a 25 mm RF insert on a Bruker DMX spectrometer (Bruker Biospin) coupled to a wide-bore magnet (dia. 89 mm) operating at 9.4 T (400.13 MHz for protons). Typical RARE images had a voxel resolution of 100x100x100 μm,) and the analyses were performed using 512 matrix TIFF images. For all marine species, as well as *Trachemys scripta elegans* and *Malaclemmys terrapin*, submillimeter, ultrahigh resolution computerized tomography (UHRCT) images were obtained on a Siemens Volume Zoom CT scanner at the Woods Hole Oceanographic Institution Imaging Facility. Marine species were obtained postmortem after death by natural causes. A spiral protocol was employed with 120 kV, 100 mA, 150 effective mAS, 0.5 mm collimation, 0.5

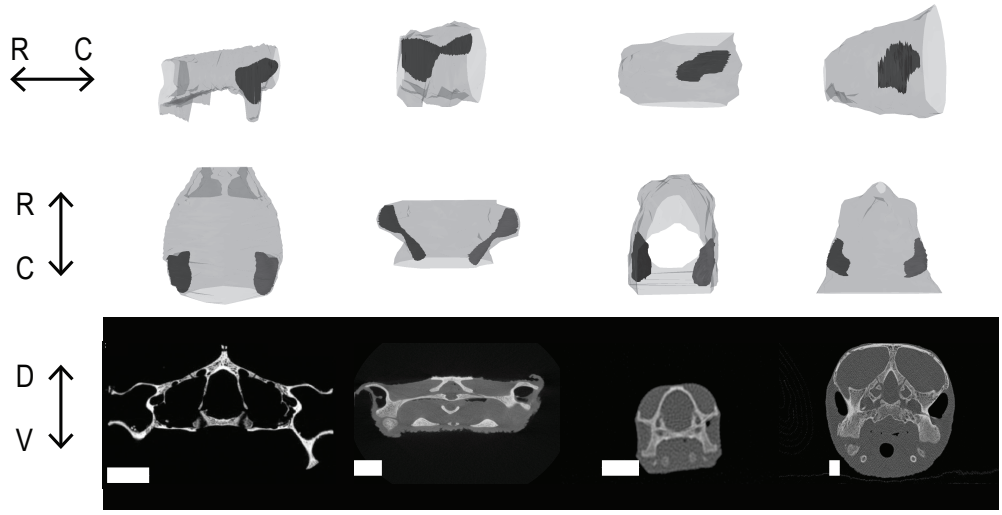

Figure 2. Examples of middle ear morphology of extant turtles and tortoises.
Middle ear cavities are in black with skulls in gray.
Top row: Lateral view of the left side.
Middle row: Dorsal view.
Bottom row: Cross section CT images at the level of the middle ear cavity.
Species in columns from left to right: *Gopherus polyphemus*, *Chelus fimbriatus*, *Trachemys scripta elgans*, *Lepidochelys kempii*.
Scale bars = 1 cm. R = rostral. C = caudal.D= dorsal. V = ventral.
Note that *G. Polyphemus* was scanned as only a skull.

mm/sec table feeds and a 0.5 mm table pitch. Both live (physically restrained) and post-mortem turtles were scanned prone, head-first, with scans acquired in the transaxial (shorter cross-section) plane. Images were reconstructed using soft, ultra-high bone, and lung kernels at 0.1 and 0.5 mm increments for the whole head and data based magnifications at smaller FOV of the ear regions alone. The 0.1 mm images provided image data sets with isotropic 100 μm voxel resolution, which were used for volume measurements and cavity reconstructions in 3D. Raw attenuation data and all 512 matrix DICOM images were archived onto CD and magneto-optical disks. In each of these programs, tissues were selected for auto-segmentation based on Hounsfield Unit values for tissue attenuations and air space attenuation. The auto-segmentations were reviewed visually and segmentation boundaries corrected when they incorporated inappropriate adjacent regions.

For all other species, CT images were obtained from DigiMorph (University of Texas, Austin). The images were 1024x1024 16-bit TIFF format. Scan parameters varied some depending on the specimen. A typically example follows: P250D, 420 kV, 1.8 mA, one brass filter, empty container wedge, 190% offset, integration time of 64 ms, slice thickness was 0.5 mm, S.O.D. was 698 mm, 1400 views, one ray averaged per view, one sample per view, interslice spacing of 0.4 mm, field of reconstruction of 268 mm (maximum field of view 280.1441), reconstruction offset of 6100, reconstruction scale of 3200. Ring-removal processing was based on correction of raw sinogram data using IDL routine ‘‘RK_SinoRingProcSimul’’ with parameter ‘‘BESTOF5.’’ This is a standardized process done for all CT scans by the imaging facilties. For an overview of the analysis of CT images, see [43]. The extinct

species used were *Galianemys emringeri* (sample ID: AMNH 30035), *Galianemys whitei* (sample ID: AMNH 29987), *Nichollsemys baieri* (sample ID: TMP 97.99.1), and *Hamadachelys escuilliei* (sample ID: MDE-T-03).

2.2 Analysis

All scan files were converted to TIFF stacks and imported into Neurolucida (MicroBrightField Bioscience, Williston, VT). For species that were scanned using both MR and CT, all data sets were used. The outlines of the structures were all traced manually in serial sections. In CT scans, the lateral edge of the middle ear cavity was defined by connecting the most medial points of bone in images where the cavity was open with a straight line. In images where the soft tissue was visible, that line was drawn through the middle of the tympanic disk. Since some the CT images usually did not include the soft tissue tympanic disk, a straight line across the opening was the best approximation. These tracings were analyzed using the NeuroExplorer module to calculate the enclosed volume. Reconstructed area is accurate to one micrometer (MicroBrightField stated accuracy). Head widths were measured as a straight line across the widest part of the head, accurate to 0.1 micrometer. Approximate head widths were confirmed as the same with calipers when possible. Resonance was calculated by modeling the middle ear cavity as an air-filled sphere vibrating underwater using the following equation:

$$F_{res}=(0.327)/[(3\times\text{volume})/(4\pi)]^{1/3}$$

(frequency in Hertz) (Urick, 1983).

Because the frequencies in question are low, and therefore the wavelengths much larger that the dimension of the cavity, the cavity can be treated as a lumped

element with a resonance frequency that only depends on volume. Univariate ANOVA tests were performed with the middle ear cavity volume co-varying with head width data categorized by ecological niche and phylogenetic position (Table 2.1). Ecological niche was defined by the medium in which the species spends the majority of its life. We divided the non-marine species according to how much time they spent in the water, in order to perform a univariate ANOVA test among the ecological niches. Animals that spent the majority (greater than 60%) of their time in non-marine environments (e.g. pond turtles) were categorized as aquatic. Sea turtles were categorized as marine. Animals spending the majority of their time on land (e.g. tortoises) were categorized as terrestrial. Those species spending approximately equal amounts of time on land and water were categorized as ‘‘dual’’. We divided the Crypotodirae into superfamilies (Trionychidea, Testuinoidea, Chelonioidea), in order to perform a univariate ANOVA test among the phylogenetic groups. Phylogentic position was determined according to the species information from the University of Michigan Museum of Zoology (Myers et al, 2012. Ecological niches were from the descriptions by (van Dijk et al., 2011). We analyzed Pleurodirae as one group because of the small number of species available and because there are far fewer extant species relative to the cryptodires.

Experiments were performed according to the guidelines approved by the Marine Biological Laboratory (Woods Hole, MA, USA), the University of Maryland Institutional Animal Care and Use Committees (IACUC) and the Danish National Animal Experimentation Board (Dyreforsøgstilsynet).

3 Results

3.1 Anatomy

In all species examined, the Eustachian tubes were small and opened adjacent to the tympanic disk on the ventral wall of the middle ear cavity, connecting the cavity to the pharynx (Fig. 2.1) (Wever & Vernon, 1956). We used *Trachemys scripta elegans* as an example species for some more detailed anatomical studies. In *T. scripta elegans*, the Eustachian tubes are narrow but detectable on MR images (Fig. 2.1 C). The fluid-filled tube appeared as a grey duct, because the middle ears were filled with saline postmortem to optimize the image. At the opening of the Eustachian tube from the middle ear, on one sample of T. scripta elegans, the tube measured about 500 mm in diameter. All species examined had middle ear cavities in the general form of paraboloids with the long axis oriented rostrocaudally, parallel to the midline (Fig. 2.2).

3.2 Allometry of Middle Ear Cavity Volume in *Trachemys scripta elegans*

In order to assess changes over the lifespan of an animal, an allometric series of 5 Red-eared Sliders (*T. scripta elegans*) was analyzed separately from the other species (Willis, Potter, & Carr, 2011) (Fig. 2.3 B) and included in the whole data set (Fig. 2.3 A).

For *T. scripta elegans*:
$\log(\text{cavity volume}) = 3.46 \times [\log(\text{head width})] - 5.7$
$r^2 = 0.89$

showing that, during the growth of an animal, head size increases allometrically with body size. From visual inspection, the overall shape of the cavity did not change with the body size.

3.3 Cross-Species Comparison

In the 25 species from 12 families examined (Table 1), the middle ear cavity was a paraboloid (Fig. 2.2) that scaled with head size (Fig. 2.3).

The scaling followed the equation:
$\log(\text{cavity volume}) = 2.4 \times [\log(\text{head width})] - 4.2$
$r^2 = 0.92$

The exception to this morphology was the Matamata, *Chelus fimbriatus*, which has a hyperboloid (hourglass-shaped) middle ear cavity, which also scaled following the above equation (Fig. 2.2). *C. fimbriatus*, is a pleurodire (Side-necked Turtle) and inhabits the Amazonian river basin. Its skull is dorsoventrally flattened, and its unusual skull morphology may constrain middle ear cavity dimensions.

The wavelengths of the sound range in question are much greater than the dimensions of the cavity and thus the effects of the shape of the cavity are negligible (Urick, 1983). Because the volume of the cavity is the primary factor for acoustic characteristics of the middle ear cavity at frequencies relevant to testudines, we used a sphere equal to the measured paraboliod volume for resonance calculations for each middle ear cavity (Urick, 1983).

3.4 Scaling and Morphology

We compared the scaling of the middle ear cavity volumes, with head width as a covariate, among the ecological groups, using univariate ANOVA, and found no significant differences ($p = 0.494$, model 2 regression $r^2 = 0.942$). When the scaling of the middle ear cavity volumes with head width was compared among the phylogenetic groups by using univariate ANOVA, no significant

differences were found ($p= 0.282$, model 2 regression $r^2 =0.773$).

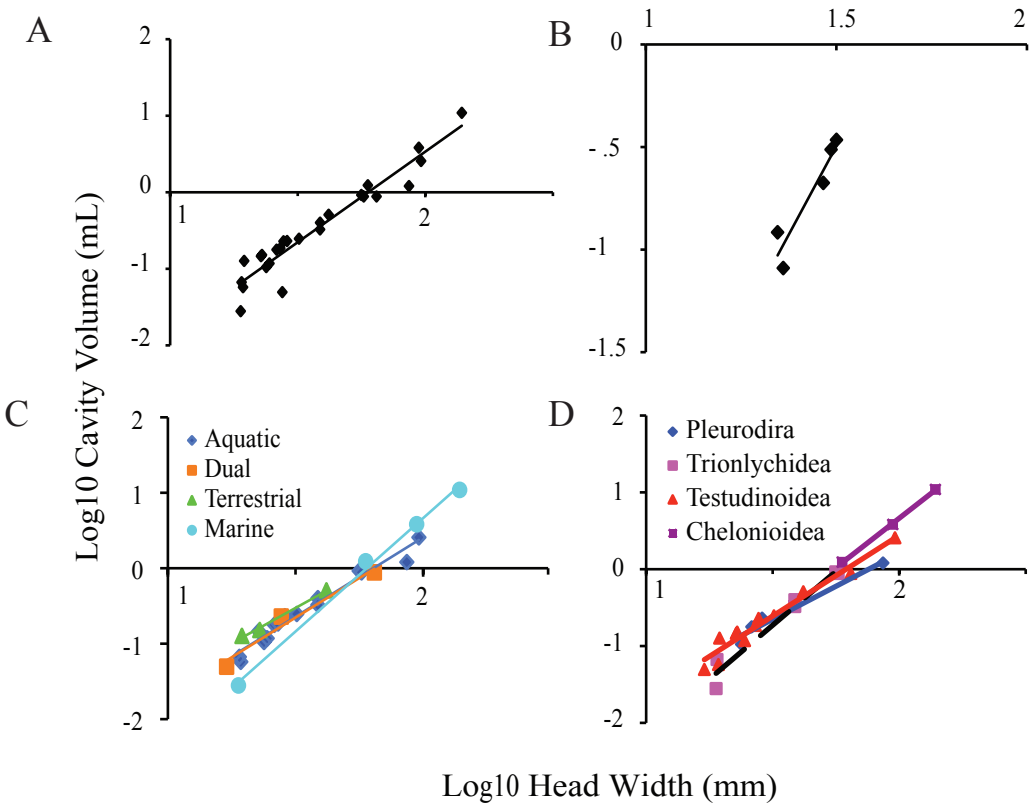

Figure 2.3. Allometry of middle ear cavities.
A: Scaling of middle ear cavity volume and head width across extant testudines
B: Scaling of volume and head width in *Trachemys scripta elegans*. C: Scaling of middle ear cavity volume and head width across extant testudines divided by ecological niche.
D: Scaling of middle ear cavity volume and head width across extant testudines divided by phylogenetic position.

3.5 Middle Ear Cavity can Function as a Resonator

Calculations were performed for a model of an air-filled sphere vibrating in an underwater sound field (Urick, 1983). Unlike the ears of lepidosaurs and archosaurs, testudine ears are not acoustically coupled (Christensen-Dalsgaard et al., 2012) and because the wavelengths are large compared with the size of the cavity, calculations were based only on the volume of the middle ear cavity. Middle ear cavities ranged in volume from 0.03 mL to 10.9 mL; head widths ranged from 19– 140 mm (Fig. 3). By modeling the middle ear cavity as a sphere vibrating underwater, we calculated the resonance frequencies of the cavities as ranging from 240–1740 Hz (Fig. 4).

3.6 Sea Turtles (Family Cheloniidae)

Sea turtle middle ear cavities contain varying amounts of fatty tissue adjacent to the tympanic disk, even differing bilaterally within the same animal (Ridgway et al., 1969; Wever, 1978). The amount of fatty connective tissue, and therefore the amount of residual air space in the middle ear, varied among the Sea Turtles examined, which complicated resonant frequency calculations. Because we were unable to determine what the exact volume of the middle ear fats might be and to what extent they compress with depth, our calculated resonance frequencies might be lower than the actual resonance frequencies experienced by the sea turtles (smaller effective resonating volume results in higher resonance frequencies). However, to date no measurements of the maximal or minimal volumes neither for these fats nor

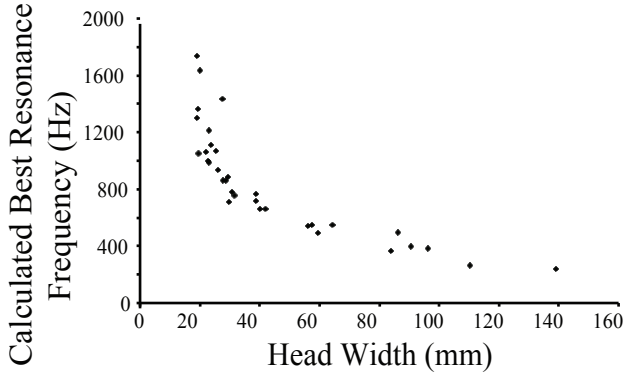

Figure 2.4. Calculated best resonance underwater frequency of middle ear cavities of extant species, changing with head size.

of their elasticity or compressibility have been published. Scans of both live and post-mortem sea turtle specimens demonstrate that the space occupied by soft tissue in the middle ear cavity can vary between individuals and even bilaterally within the same turtle, but we do not know whether these variations remain underwater. In the absence of such data, we calculated the maximal cavity volume based on skull morphology. Based on the skull structure, the allometry of the middle ear cavity of sea turtles did not scale differently from the other testudines (Fig. 3.3 C, D).

3.7 Extinct Species

CT scans of several extinct species, including *Galianemys emringeri, Galianemys whitei, Nichollsemys baieri,* and *Hamadachelys escuilliei*, revealed that *Galianemys* and *Hamadachelys* species have middle ears that are connected through the mouth, to the extent observable from the fossilized remains (Fig. 3.5), while *Nichollsemys baieri* has more isolated ears, like the extant testudines (Fig. 3.2). In the CT images of the *Galianemys* and *Hamadachelys* species, there is a clear opening from the middle ear cavity into the mouth (Fig. 3.5 C). This large opening is not seen in N. baieri. As the Eustachian tubes are comprised of soft tissue, the size of the Eustachian tubes could not be determined. Connected ears were also shown in *Proganochelys* (Gaffney, 1983). These specimens were not reconstructed in detail, nor used for volume calculations, because of the potential distortions derived from fossil compression. *Galianemys emringeri, Galianemys whitei, Nichollsemys baieri* were pleurodires, and *Hamadachelys escuilliei* a cryptodire. All of the specimens were found in Cretaceous formations.

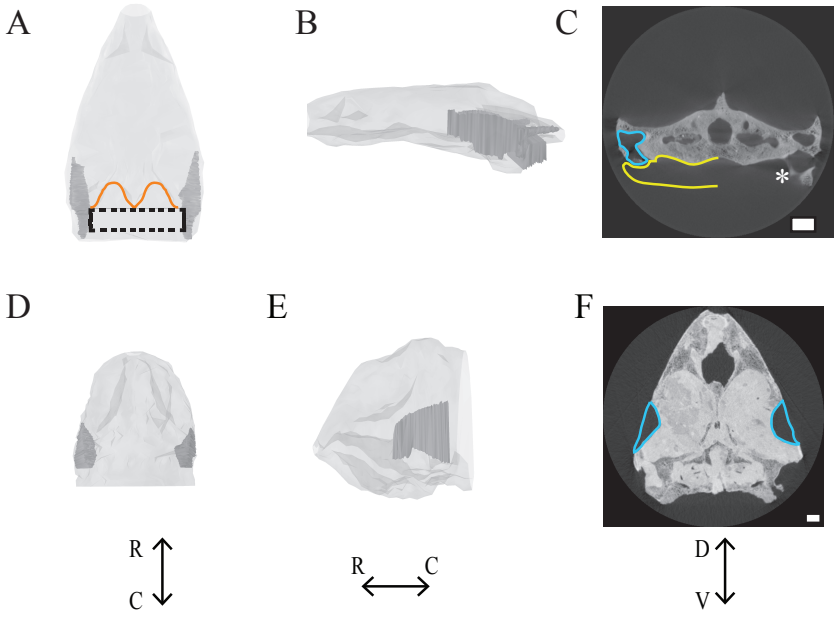

Figure 2.5. Examples of middle ear cavities of extinct testudines.
A-C: Connected ears of Galianemys emringeri. Connected middle ears are shown in dark gray; the skull is shown in light gray. The maximum space that the connected middle ears could possibly occupy is indicated by the dashed line. The dorsocaudal edge of the skull is outlined in orange.
D-F: Separated ears of Nicholsemys baieri. Isolated middle ears are show in dark gray; skull is shown in light gray.
A & D: Dorsal view.
B & E: left lateral view.
C & F: Transverse view from CT.
Middle ear cavities are outlined in blue, and possible extent of middle ear cavity into pharynx is yellow. Asterisk indicates most caudal part of the middle ear cavity that can be seen intact before it opens into the pharynx.
Scale bars = 1 cm. R = rostral. C = caudal. D= dorsal. V = ventral.

4 Discussion

4.1 Middle Ear Cavities Enhance Hearing

Resonance via enlarged middle ear cavities has been shown to affect hearing in a number of vertebrate classes, both in air and under water. For example, the enlarged middle ear cavity of kangaroo rats underlies good hearing thresholds below 3 kHz, particularly in the 1–2 kHz range (Ravicz & Rosowski, 1997; Webster, 1962). Similarly, the bulla (middle ear cavity) in gerbillines acts like a Helmholtz resonator, lowering hearing thresholds (Plassmann & Kadel, 1991). One example of air-filled structures lowering hearing thresholds underwater is Ostariophysan fishes, which couple swim bladders to Weberian ossicles, enabling sound pressure hearing, not just detection of particle motion (Evans, 1925; Polgar et al., 2011; Webb et al., 2006; Zeddies, 2005). Similarly, the ranid frog *Lithobates (Rana) catesbeiana* is more sensitive to sound below 200 Hz underwater than in air and is equally sensitive in air and in water for frequencies above 400 Hz, possibly due to specialization of the amphibian papilla (Lombard et al, 1981). The middle ear cavity of the African clawed frog (*Xenopus laevis*) provides hearing advantages underwater (Christensen-Dalsgaard & Elepfandt, 1995). The ear of *Xenopus* works like the turtle ear, with cartilaginous tympanic disks and an air-filled resonating cavity. Xenopus also has further adaptations for underwater hearing, including a tighter coupling and lower lever ratio between the tympanic disk and ossicles than do the ranid frogs (Mason et al., 2009).

Wever and Vernon were aware of the potential for middle ear resonance in their studies of turtle hearing (Wever & Vernon, 1956). They calculated resonance

frequencies for the middle ear cavities in *Chrysemys picta picta* and *Trachemys (Pseudemys) scripta* in air to be 6 kHz by using a closed tube model where the resonance frequency quarter wavelength matches the length of the tube. Volumes used in obtaining this value were not published. Because 6 kHz was well above measured highest audible frequency (about 2 kHz), they discounted any increased sensitivity modeling based on resonance. Recent studies, however, show that the ear of *Trachemys scripta elegans* is more sensitive to sound underwater than in air (Christensen-Dalsgaard et al., 2012), where resonance frequencies are much lower. We hypothesize that the conserved structure of the testudine ear is an adaption for underwater hearing that was retained by neutral selection.

Middle ear cavities are also interesting from the perspective of understanding how a major vertebrate group processes sound. Hearing has been documented in multiple species of testudines, demonstrating that these animals have auditory sensitivity, albeit with higher thresholds in air than those of other reptiles (Wever, 1978). Six testudine species have published in air audiograms (Table 2.2), with best hearing frequencies below 1000 Hz (around 400–600 Hz).

There is much to be learned about how the testudine middle ear responds to sound underwater. Laser vibrometry studies, perhaps from post-mortem samples from a variety of species, could be used to test the hypothesis that both turtle and tortoise ears would respond well to underwater sound. The fossil specimens without isolated middle ear cavities could represent either the ancestral diapsid condition, or a secondary loss. As more extinct species are discovered, answers to this question should become clearer.

4.2 Sea Turtle Ears

The function of the fatty tissue in sea turtle middle ears is unknown, while the high degree of variability in these structures adds to the mystery. There are a variety of hypotheses about their function, including their being an adaptation to the pressure resulting from deep diving (Ridgway et al., 1969; Wever, 1978), or a secondary pathway for sound transmission, in a manner analogous to the fatty channels in the jaws of marine mammals (Ketten et al., 1999). While our data do not address the function of this tissue, they do suggest that fatty tissue in the middle ear may be secondary adaptation in sea turtles, because their skull elements and allometry are the same as the other testudines.

4.3 Phylogenetic Position of Testudines

As shown by Christensen-Dalsgaard and colleagues, at least one species of turtle has lower under water hearing thresholds than in air, largely due to the middle ear cavity (2012). Given that the middle ear cavity resonates underwater within the published in-air testudine hearing range and that the middle ear cavity resonates beyond that range in air (Wever & Vernon, 1956), our findings of unchanging middle ear cavity allometry among the testudines support the hypothesis of an aquatic origin for this group. Since the tortoises retained this allometric relationship, we further hypothesize that the middle ear cavity does not impede hearing in air. Analyses of the hearing of testudines have been complicated by their ill-defined relationship to other major vertebrate groups. Since testudines are anapsids, they had been considered an extant representative of the parareptiles, which places them as a sister to the entire diapsid clade. This position was supported by some morphological analyses

Species	Lowest Tested Frequency (Hz)	Highest Tested Frequency (Hz)	Best Frequency Range (Hz)	Reference
Chelonia mydas	30-40	2000	300-400	Ridgway, et al (1969)
Clemmys insculpta	100	5000	500	Wever & Vernon (1956c)
Chrysemys picta picta	100	4000	400-500	Wever & Vernon (1956c)
Caretta caretta	250	1000	250-500	Bartol et al (1999)
Terrapene carolina carolina	30	4000	400	Wever & Vernon (1956b)
Trachemys scripta elegans	100	3000	500	Wever & Vernon (1956c)
Trachemys scripta elegans	100	1000	400-500	Christensen-Dalsgaard, et al. (2012)

`Table 2.2: Published testudine in-air audiograms.

(Lee, 2001; Lyson et al., 2010). Rieppel and deBraga, however, proposed that testudines are the sister group to lepidosaurs (1996). They state that the traditional view, in

which the number of temporal fenestra is the deciding factor for determining vertebrate relationships, is too narrow. Their analyses included a much wider range of non-skull characters (Rieppel & deBraga, 1996). A recent study of mesosaurid skulls supports diapsid affinities of the testudines (Piñeiro et al., 2012). Interestingly, data that support testudines being either the sister group to the archosaurs or to the entire diapsid clade support a terrestrial origin of testudines (Lyson et al., 2010); conversely, the data that support testudines being the sister group to lepidosaurs support an aquatic origin (Rieppel & Reisz, 1999).

The advent of molecular techniques and the application of these methods to phylogenetic problems called into question the traditional understanding of the position of testudines. Phylogenomic analyses have led to a reevaluation of the position of the testudines. These studies robustly support the position of testudines as sister to the archosaurs, with the archosaurs remaining monophyletic (Crawford et al., 2012; Shen et al., 2011). Hedges and Poling found that in all but one gene, testudines were most closely related to archosaurs (1999). The position of testudines within the diapsid clade has been supported by other molecular analyses (Chiari et al., 2012; Iwabe, 2005; Mannen & Li, 1999; Zardoya & Meyer, 2001). While our data do not directly address the phylogenetic position of testudines, they support an aquatic origin for this group. There is also support for this claim from the fossil record: Odontochelys, the most basal testudine discovered thus far, appears to have been

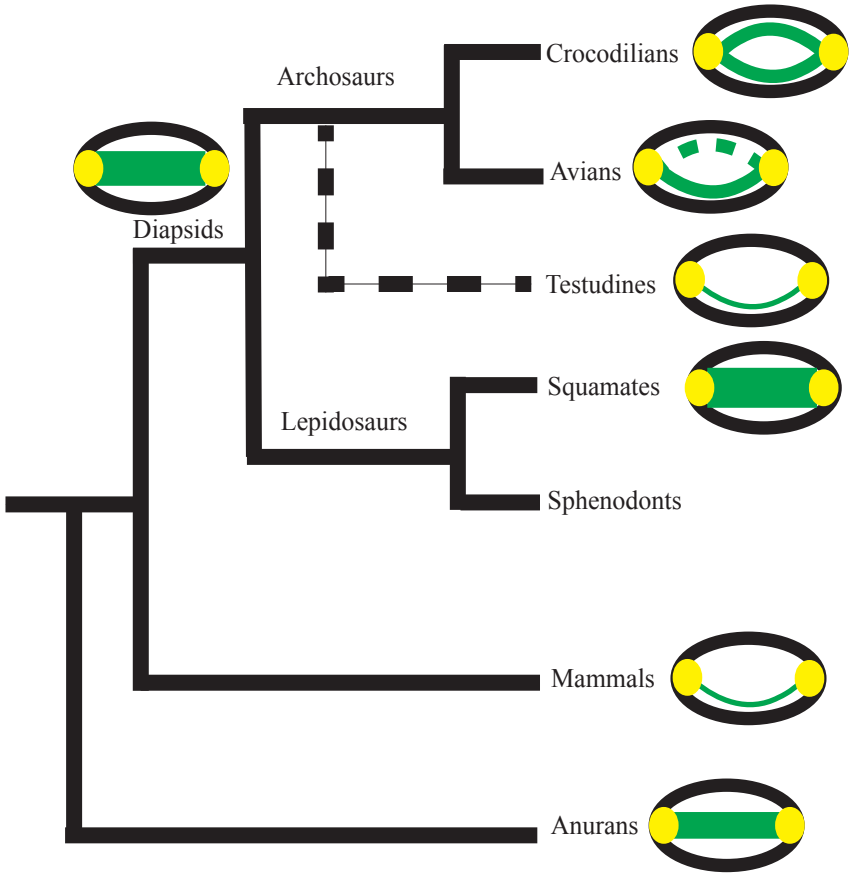

Figure 2.6. Proposed middle ear structure across some extant vertebrate taxa. Skulls are shown in black, tympanic ears in yellow, connections between the ears (Eustachian tubes or through the buccal cavity) in green. The dashed line on the avian diagram indicates trabeculated bone. The proposed diapsid ancestral condition is also shown. The dashed branch to testudines indicates their suggested phylogenetic position

aquatic (Li et al., 2008). A parsimonious explanation is that the common ancestor of archosaurs, lepidosaurs, and testudines had coupled ears that opened into the pharynx, since coupled ears are the ancestral condition for tympanic ears (Fig. 6) (Christensen-Dalsgaard & Carr, 2008; Clack, 2002). Our data suggest that Testudines secondarily evolved acoustically isolated middle ear cavities because of the improved underwater sound sensitivity that they provide.

4.4 Conclusions

After separating species by ecology and phylogeny (Fig. 3.4), no significant differences in the variation of middle ear cavity volume and head width were observed, suggesting that there has been little modification among extant testudines. Since middle ear cavities enhance hearing under water (Christensen-Dalsgaard et al., 2012), testudines should have lower hearing thresholds in water than in air. A lower hearing threshold under water than in air could only theoretically apply to the terrestrial species. Since not all extant testudines are aquatic or amphibious, the most probable explanation for this constancy is that neutral selection has maintained middle ear cavity scaling.

Given constancy in middle ear cavity scaling, we hypothesize that the most recent common ancestor of the extant testudines was primarily aquatic and had separated middle ears, an assertion supported by two observations from the fossil record. First, in some extinct species of testudines, including *Galianemys emringeri, Galianemys whitei*, and *Hamadachelys escuilliei*, the middle ear cavities opened into the mouth, as does the internally coupled, pressure difference receiver ear of lizards (Christensen-Dalsgaard & Manley, 2008; Tang et al., 2012). Christensen-Dalsgaard

and Manley have argued that coupled ears are both the simplest configuration of, and the ancestral condition for, tympanic ears (Fig. 3.6) (Christensen-Dalsgaard & Manley, 2008). Second, isolated middle ear cavities appeared in both the extinct marine cryptodire, *Nichollsemys baieri* (Brinkman, 2005), and independently in the mosasaurs (marine lizards) (Hetherington, 2008). The evolution of isolated middle ear cavities in testudines would have provided some selective advantage, which we hypothesize was an increased sensitivity for conspecific vocalizations and auditory scene analysis in a primarily aquatic habit, which may then have been retained by neutral selection.

5 Acknowledgements

The authors acknowledge J. Arruda, C. Bell, D. Brinkman, K. Catania, S. Cramer, E. Gaffney, H. Jamniczky, J. Maisano, and K. Potter for assistance with scans and specimens, and H. Bierman, D. Hertz, R. Highton, T. Holtz, J. Merck, and D. Soares for advice and discussion. We thank the anonymous reviewers for their helpful comments.

Chapter 3: Towards a Detailed Anatomical Characterization of the Turtle Auditory Brain Stem Circuit

The anatomy and tract tracing portions of this chapter are currently in preparation by K.L Willis and C.E. Carr for submission to a journal. The statistical analyses and application in this chapter are currently in preparation by K.L Willis, J. Chrabaszcz and C.E. Carr for separate submission to a journal

1 Introduction

Hearing is used by organisms for a variety of behaviors and generally mediates sensitivity to both the auditory scene and to communication sounds. Sensitive hearing requires both specialized ear structures and neural processing (reviewed in Willis et al., 2013b, chapter 1, this dissertation). Ear structures include the tympanum, an adaptation to hearing in air. Tympanic hearing can be traced through the fossil record (Clack, 2002) and has evolved at least 3 times, in the lineages leading to modern amphibians, reptiles and mammals (Clack, 1997).

The hearing of turtles and tortoises (collectively Testudines) has not been commonly studied, in part because turtles hear lower frequencies, mostly below 1 kHz, and are thus not regarded as auditory specialists (Christensen-Dalsgaard et al., 2012, Table 2.1, review in Manley, 2010). Turtle hearing capabilities are nevertheless interesting, since turtles have recently been identified as a sister group to the archosaurs (Lu, Yang, Dai, & Fu, 2013), which have well developed hearing. I have therefore described the turtle auditory system in order to compare it with that of other reptiles.

In all reptiles, including birds, the auditory branch of cranial nerve VIII bifurcates to terminate in the nucleus magnocellularis (NM) and the nucleus angularis

(NA). NM projects bilaterally to the nucleus laminaris (NL). NL and NA then project to the midbrain torus semicircularis (Carr & Boudreau, 1991; Takahashi & Konishi, 1988; Tang, Christensen-Dalsgaard, & Carr, 2012; Young & Rubel, 1983). Previous work on turtles has shown that the auditory branch of the VIII nerve also projects to NM and NA (Marbey & Browner, 1985; Sneary, 1988). A difficulty in many of these older studies, however, lies in the identification of nuclear borders. For example, Miller and Kashara (1979) were not able to identify a clear NM to NL projection, or differentiate between NM and NL.

We have therefore used modern techniques to define the auditory nuclei and their connections. We have also used mathematical analyses to determine whether there are distinct cell types within each nucleus. We hypothesize that connections among the auditory nuclei in the turtle will follow the reptile pattern, but show less specialization, since turtles are sensitive to low best frequencies.

2 Materials and Methods

All experiments were carried out with the approval and under the guidelines of the University of Maryland Institutional Animal Care and Use Committee.

2.1 Surgery and Anesthesia

Adult Red-eared Sliders (Trachemys scripta elegans) of both sexes were obtained from Kon's Direct (Germantown, WI). Animals were group housed and maintained on a 12 h light cycle. Propofol (5mg/kg) was administered intravenously. After cessation of all reflexes, including eye blink, animals were rapidly decapitated. The brain was exposed from the rostral spinal cord up to the midbrain to allow for

exposure to oxygenated artificial cerebrospinal fluid (ACSF). ACSF was comprised of 96.5mM NaCl, 2.6mM KCl, 4.4mM CaCl2, 2.0mM MgCl2, 31.5mM NaCO3, and 10mM dextrose, dissolved in double distilled water (Connors & Kriegstein, 1986; detailed in chapter 4). The middle ear cavity, inner ear cavity, and skull were opened to expose the basilar papilla, auditory branch of VIII nerve, and other landmark structures. The cerebellum was removed to allow for visualization of the acoustic tubercles.

2.2 Tract Tracing

Two methods of dye injection were used. In some cases, Neurobiotin (NB, Molecular Probes, WA) was placed on the tip of a minutin pin and applied to the basilar papilla, auditory branch of VIII nerve, or brain stem or midbrain structures. Alternatively, 1.5% NB, dissolved in 0.5M NaCl (with Fast Green added for visualization) was injected into either the basilar papilla or VIII nerve using iontophoresis. A 3 μA positive current was passed for 10 minutes in 7 s on/7 s off pulses. The electrode was left in place for 10 minutes after the current was turned off. Biotinylated dextran amine (BDA) (Life Technologies) was pressure injected.

In order to allow for dye transport, the tissue was maintained in a 4°C refrigerator, with oxygen-saturated ACSF changed every 24 hours. Transport time varied from 48-96 hours depending on location and dye type. The brain was then removed and fixed in 4% paraformaldehyde in 0.01M phosphate buffered saline (PBS) for 18-24 hours. The brain was then cryoprotected in 30% sucrose in 0.01 M PBS solution until completely permeated.

Tissue was cut on a freezing microtome in 80 μm sections, and then rinsed in 0.01 M PBS. Sections were submerged in ABC (Vector Labs), in a 2% Triton in 0.01M PBS solution for 2-4 hours at room temperature. Following rinsing in 0.01M PBS, the tissue was reacted with the SG kit (hydrogen peroxidase and chromagen) (Vector Labs) until the enzymatic reaction was sufficiently dark. SG solution was then rinsed off with 0.01M PBS.

Processed tissue was mounted on gelatin-subbed slides, maintaining order along the rostro-caudal axis. After drying, it was counterstained with neutral red or cresyl violet for visualization purposes. Tissue was dehydrated with an ethanol series followed by Xylene. Cytoseal was then used for coverslipping the slides.

2.3 Rapid Golgi and neuronal reconstruction

Digital reconstructions of labeled neurons were carried out using NeuroLucida (MBF Bioscience). The outline of the entire brain stem was also reconstructed. Individual labeled neurons were drawn at 100x. These digital reconstructions are such that the details of the three-dimensional structure of the neuron were preserved and measured. For Rapid Golgi, animals were sacrificed, and the brains were removed and placed in Golgi fixative containing potassium dichromate, mercuric chloride and potassium chromate (Rapid Golgi kit, FD NeuroTechnologies, Ellicott City, MD), then sectioned in the transverse plane. Labeled neurons were reconstructed as above.

2.4 Analysis

Measurements of neurons were carried out using NeuroExplorer (MBF Bioscience). These factors were compared using multidimensional scaling among

NA, NM, and NL, as well as within each nucleus (for details on multidimensional scaling see Kruskal, 1964). Multidimensional scaling is a technique for collapsing high-dimensional data into an arbitrarily smaller number of dimensions. This is done by finding distances between each object in high-dimensional space (in this case Euclidian distance) and then minimizing error in the specific number of dimensions for those distances. In our case, we have neurons that differ on a number of outcomes, (e.g., size, roundness, degree of dendritic arborization). We generated a set of differences between each pair of cells based on the various cell measurements and then projected these differences onto a two-dimensional set of scores that minimized loss from the original difference pairs. The result is a scatterplot of points corresponding to each cell, with the distance between any points interpretable as the dissimilarity of those two cells.

3 Results

Using cresyl violet stain, we were able to differentiate 5 auditory nuclei (Fig. 3.1). The first order nuclei NA and NM were located in the acoustic tubercle of the brain stem. The secondary nucleus NL was also located in the acoustic tubercle, below NM. NM, NL, NA, SO, and torus semicircularis were found in similar locations to lizards and birds (Carr & Code, 2000; Willis et al., 2013b). The nuclei were also roughly the same shape as found in birds and reptiles. All nuclei run in rostro-caudal columns. NM was the most caudal nucleus. The rostral portion of NM overlapped the caudal portion of NL. NL was ventral to NM and NA. The caudal part of NA overlapped the rostral part of NL, and was dorsal to NL. NA and NM were superficial, located on the edge of the brain stem close to the IV ventricle. NM was

Figure 3.1 Cresyl Violet (Nissl) stained transverse sections. Most rostral section is in the top left, progressing to the most caudal section in the bottom right. Torus semicircularis (TS), Nucleus Angularis (NA), Superior Olive (SO), Nucleus Laminaris (NL), and Nucleus Magnocelluaris (NM) are outlined and designated on the right half of each section. 100 μm scale bars

round in transverse section. NA became more round in transverse section rostrally. Caudally, NA had less defined borders, but formed a polygonal outline in reconstructions. NL formed a crescent shape in transverse section. It was more compact medially and spread out along the dorosventral axis more laterally. The torus semicircularis formed the dorsal portion of caudal midbrain, just rostral of the cerebellar peduncles and caudal to the optic tectum. The superior olive was located in the rostral-ventral portion of the brain stem.

The auditory portion of cranial nerve VIII branched inside the brainstem (Fig. 3.2). It formed both bouton and en passant terminals on cell bodies, dendrites, and neuropil of NA and NM. The tract of the VIII nerve remained in the dorsal portion of the acoustic tubercle. We found no endbulb terminals in NM, contrary to Browner and Marbey (1988). As seen in Figure 3.2, VIII endings formed a dense neuropil on and around NM neurons, in contrast to NA, where terminals were more sparsely distributed (Fig. 3.2). Reconstructions from NB injections into the auditory branch of VIII nerve revealed terminals in NM that were not significantly larger (5.37 ± 2.3 μm2) than those on NA (5.26 ± 2.8μm2, p=0.34; NA n = 135, NM n = 220). Terminals onto NA were, however, significantly more round (form factor = 0.84± 0.07) than those on NM (form factor = 0.78±0.13, $p < 0.001$), as determined by ANOVA.

Nucleus angularis was located rostral to NM. Both NA and NM were dorsal to and partially overlapped with NL (Fig 3.1). The borders of the nuclei were distinguishable in both cresyl violet (Fig 3.1) and neutral red material. NA lay close to the surface of the brainstem below the ventricle, and caudal to the cerebellar

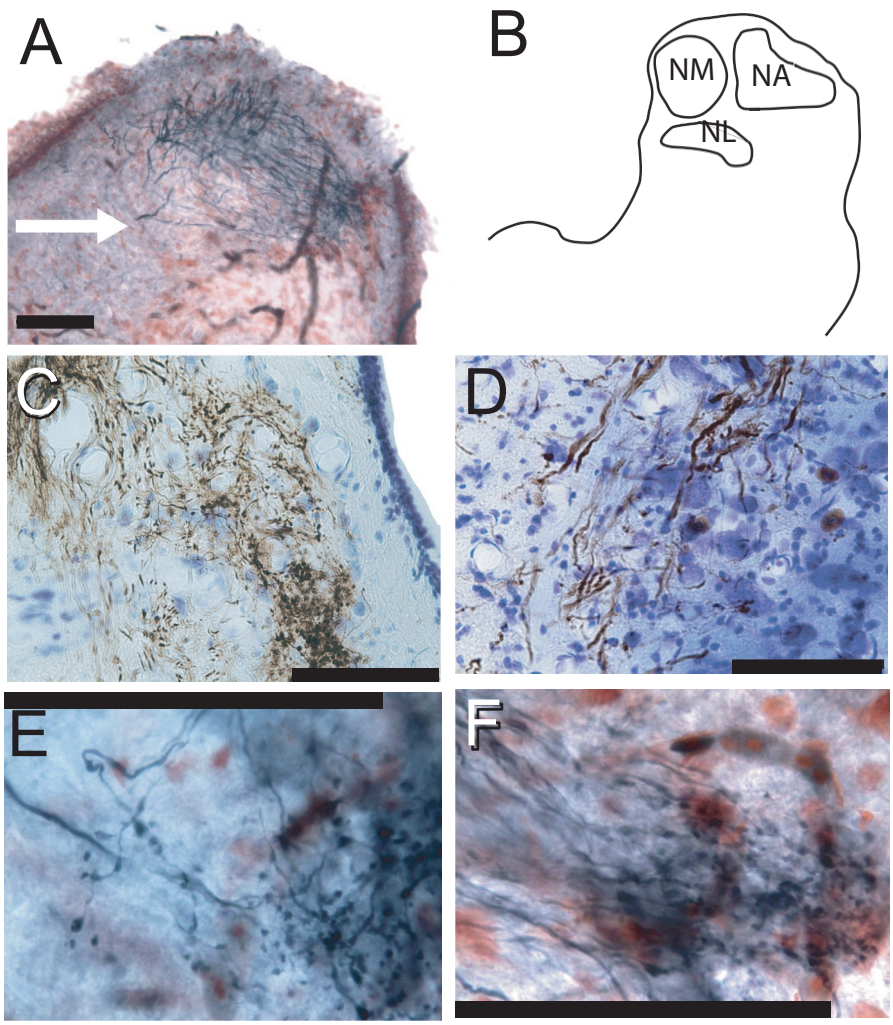

Figure 3.2 Projections of the Auditory Branch of the VIII Nerve
A. NB filled VIII nerve prjections. Arrow indicates branching point. Dorsal (top) fibers go to NA. Ventro-medial fibers go to NM. (100 ⌠m scale bar)
B. Schematic of brainstem in transverse section showing rostro-caudally collapsed relative position of NA, NM, and NL.
C. VIII nerve endings onto NM (100 ⌠m scale bar)
D. VIII nerve endings onto NM (100 ⌠m scale bar)
E. En passant terminals (100 ⌠m scale bar)
F. Bouton terminals (100 ⌠m scale bar)

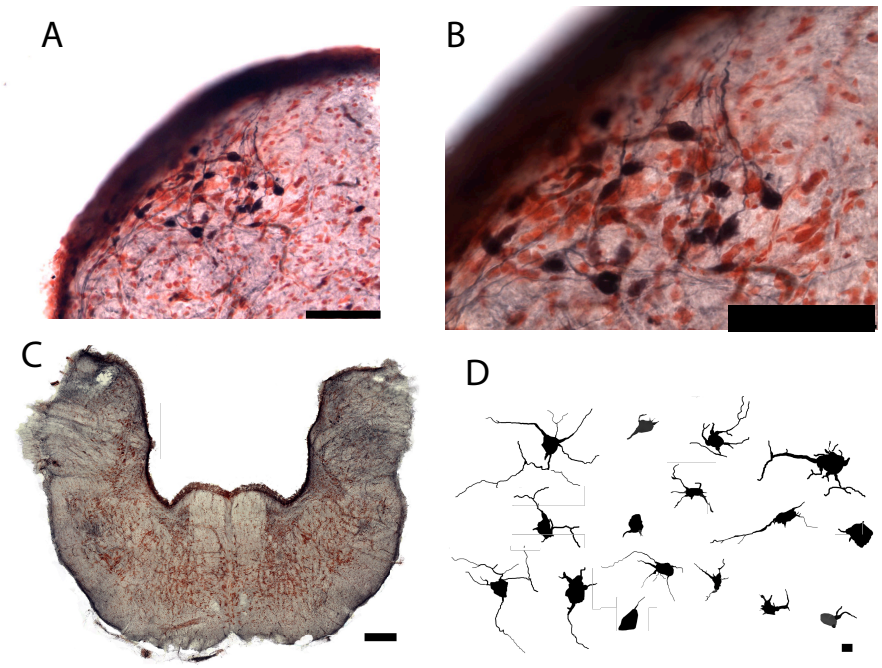

Figure 3.3. Nucleus Angularis
A. NA neurons retrogradely labeled from TS in transverse section 100 ⌠m scale bar
B. Magnified view of A. 100 ⌠m scale bar
C. NA in transverse section showing ipsi- and contralateral retrograde labeling from TS NB injection. Boxes indicate NA. 100 ⌠m scale bar
D. Reconstructed NB and Golgi labeled NA neurons. 10 ⌠m scale bar

peduncle. In addition to position, NA was defined by input from the ipsilateral VIII nerve and a bilateral projection to TS (Fig. 3.3). NA neuronal morphology (n = 43) was heterogeneous, and generally multipolar (Fig 3.3). I was unable to further classify neuronal types in NA, either visually or with analytic techniques (Figure 3.3). NA neurons varied in size, number of dendrites, and orientation. In NA, as well as NM and NL, neurons had few dendritic spines. Numerical data were combined from Golgi, BDA, and NB material. The soma of NA neurons had an average form factor of 0.79 ± 0.1. The average length of a single NA dendrite was 18.0 ±16.4 μm. The average soma area was 266.8 ± 131.6 μm^2.

NM received input from VIII nerve and projected to contra- and ipsilateral NL. NM neurons (n = 52) showed variation in numbers of dendrites (Fig 3.4). Some neurons had very short or no dendrites, while others had dorsally directed dendritic arbors that penetrated the VIIIth nerve tract above NM (Fig. 3.4). The somata of NM neurons had an average form factor of 0.85 ± 0.07. The average length of a single NM dendrite was 30.8 ± 24.8 μm. The average soma area was 139.9 ± 68.3 μm^2. Contralaterally projecting NM axons formed a distinctive cross-tract above the medial longitudinal fasciculus (Fig. 3.4). These axons ascended into the contralateral acoustic tubercle and arborized in the neuropil below the contralateral NL cell body layer.

NL projects bilaterally to TS, as seen from retrograde labeling using NB. TS additionally receives input from SO and NA. NL forms a lamina that is compact medially and spreads laterally. It is characterized by generally bitufted neurons (n =

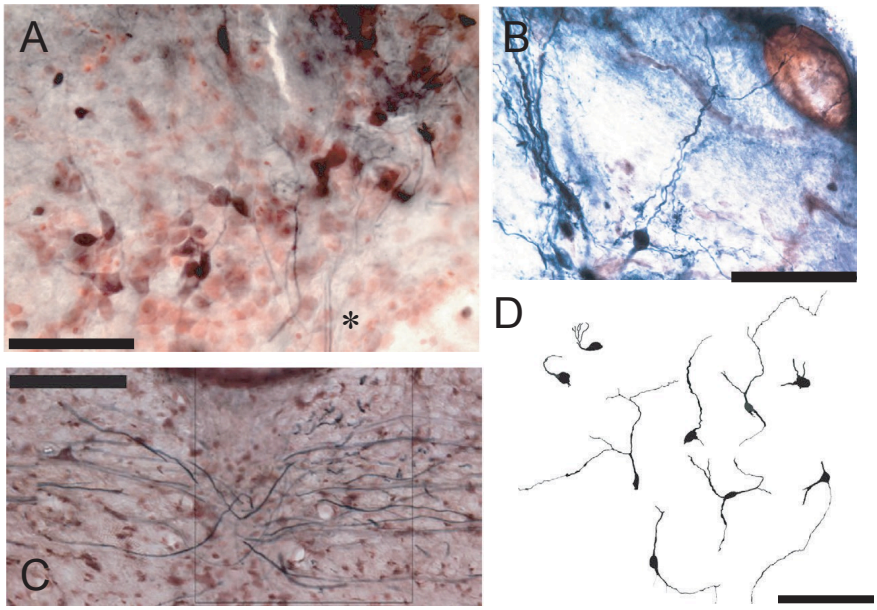

Figure 3.4. Nucleus Magnocellularis.
A. NB retrogradely labled NM neurons from NL. Soma are round. To left of * note the beginning of the crossfiber bundle. 100 ⌠m scale bar
B. NB retrogradely labled NM neurons from NL with dendrites projecting into the VIII axon tract. 100 ⌠m scale bar
C. Crossfiber bundle of NM axons at the midline projecting to contralateral NL. 100 ⌠m scale bar
D. Reconstructed NB and Golgi labeled NM neurons. 100 ⌠m scale bar

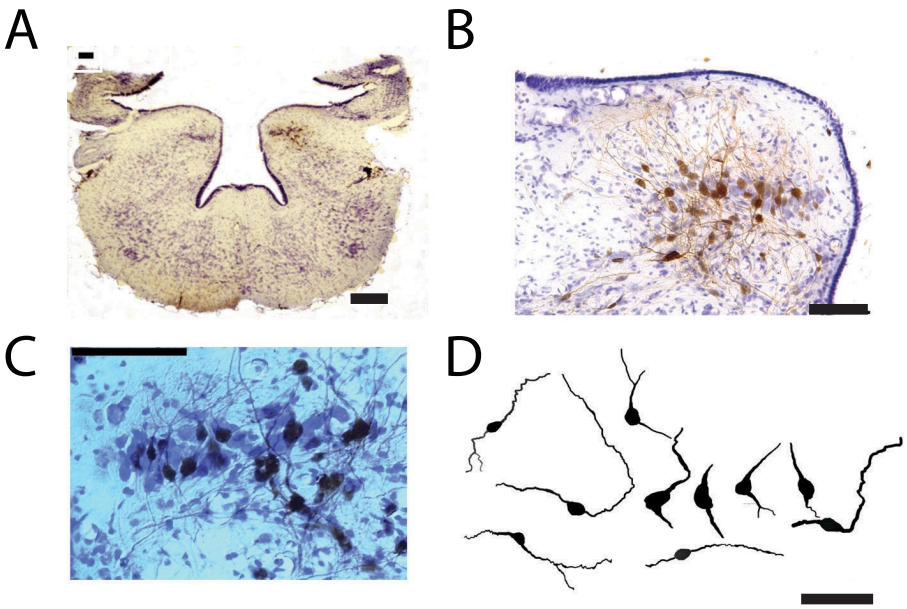

Figure 3.5. Nucleus Laminars
A. NB retrogradely labeled NL neurons. Label on left side. Counterstained with cresyl violet. Boxes indicate NL (100⌠m scale bar)
B. NB retrogradely labeled NL neurons. Magnified from A. (100⌠m scale bar)
C. NB retrogradely labeled NL neurons. Magnified from B (100⌠m scale bar)
D. Reconstrucuted NB and Golgi labeled NL neurons (50⌠m scale bar)

99). Medially, these neurons are oriented along the dorsal-ventral axis (Fig. 3.5). More laterally, neurons shift orientation and spread out dorsoventrally, while remaining largely bitufted. Neither the shift in orientation nor the dorsoventral spreading is uniform. Generally, the more lateral NL neurons are more spread out in dorsoventral space and are more likely to not be oriented along the dorsoventral axis. The soma of NL neurons had an average form factor of 0.86 ± 0.1. The average length of a single NL dendrite was 46.5 ± 29.9 μm. The average soma area was 143.5 ± 56.3 μm^2.

Using multidimensional scaling (Kruskal, 1964), we found that NA, NM, and NL populations separate along two components (Fig. 3.6). Using ANOVA, three main traits were found to be significant. NA soma areas were larger than NL or NM ($p < 0.01$). NA soma form factors were lower than NM or NL (i.e. NM and NL soma were more round, $p < 0.05$). Finally, NL average dendrite length was greater than NM or NA ($p < 0.01$). Combining many factors, using multidimensional scaling, NM, NL, and NA form separate populations (Fig. 3.6). The populations were not, however, widely separated. There were few single traits that were significantly different; NA neurons had shorter dendrites, while NA neurons had larger cell bodies.

4 Discussion

Examining the measurements of reconstructed neurons, it is clear that traits of neurons within a given nucleus are variable. Combining these observations with multidimensional scaling techniques, one sees that while NA, NM, and NL were separable, they were not widely separated. One option for differentiating neurons

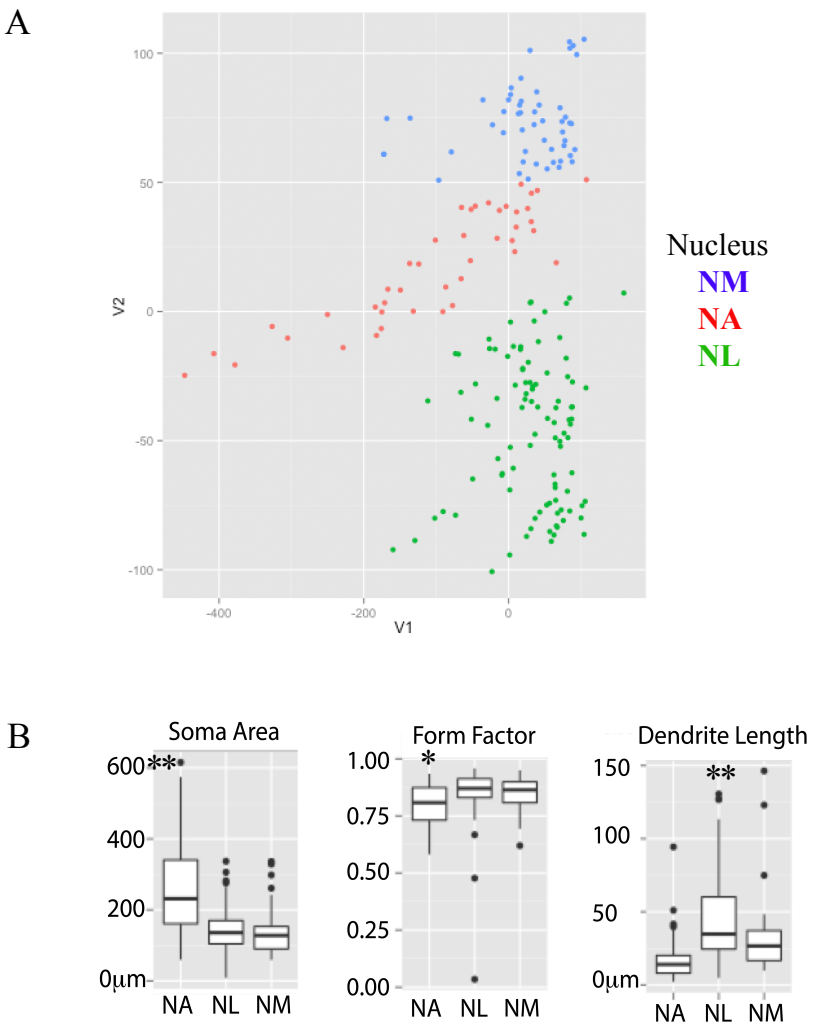

Figure 3.6 Statistical Analysis of Difference Among Nuclei
A. Multidimensional Scaling (MDS) plot of NA, NM, and NL
B. Box plots of soma area, form factor, and dendrite length.
* $p < 0.05$; **$p < 0.01$

further would be to use chemical neuroanatomy, such as immunohistochemical investigation, expanding on the work by Belekhova et al (2002), who examined calcium binding protein expression in brainstem auditory structures. She found parvalbumin, calbindin and calretinin-like immunoreactivy in NN, NM and NL. Examination of immunohistochemical profiles in each nucleus could potentially separate the nuclei from each other and may yield a clear immunohistochemical cell type within a nucleus.

One auditory system trait shared across turtle and tortoise species is that it detects only low frequencies, generally below 1 kHz (Christensen-Dalsgaard et al., 2012; Wever & Vernon, 1956; Willis, et al., 2013a). This is clear in the anatomy of the endings of the VIII axons onto NM neurons (Fig. 3.2). Although we could differentiate auditory nerve terminals in NA and NM, we did not find endbulb terminals in NM. This was contrary to Browner & Marbey's assertion (1988). The existence of boutons and not endbulbs is consistent with findings in the low frequency areas in birds, where the auditory nerve also forms boutons (Koppl, 1994). Endbulbs appear to be a specialization for phase locking at high best frequencies, by providing high-fidelity of transmission across the synapse by increasing the area for transmitter release. The turtle auditory system is characterized by low frequency hearing, hypothesized to be the ancestral condition (Christensen-Dalsgaard & Carr, 2008). We note that understanding of testudines' low frequency hearing may be complicated by their adaptation to hearing underwater (Christensen-Dalsgaard et al., 2012; Willis et al., 2013a). Since sound travels much faster under water than in air,

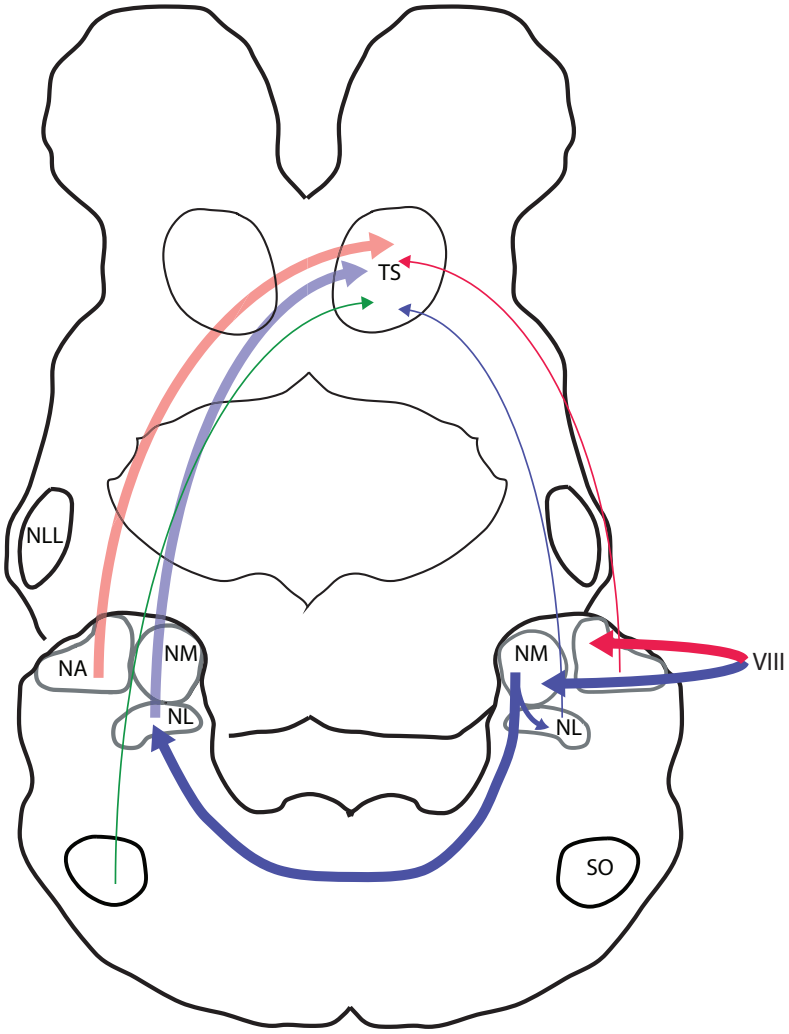

Figure 3.7. Summary of the connections among the brain stem auditory nuclei in the turtle. Red indicates the pathway from VIII nerve to NA, then bilateral projection to TS. Blue indicates the pathway from VIII nerve to NM, then bilateral projection to NL, followed by bilateral projection to TS. Green indicates the SO-TS connection. Thin lines indicate that it is a smaller relative contribution. In both the NL-TS and NA-TS pathway, ipsilateral is smaller than contralateral

hearing underwater might have effects on neural processing that may not be revealed by anatomical experiments. In birds and mammals, which generally have high-frequency hearing, the brain stem nuclei increase in size and neurons differentiate into types. This is seen clearly in the NA of birds, which contains visually distinguishable cell types (e.g.
Soares & Carr, 2001). In turtles, cell types are neither visually nor mathematically distinguishable. In NA, cells are generally heterogeneous and multipolar. Multiple theories have been put forward to explain neuronal structure-function relationships. One explanation is that specific cell types process specific types of information. Addition of high-frequency information could have resulted in selective pressure for neurons to specialize to process parallel streams of information. If this were the case, turtles can be used as a possible window into the ancestral condition.

Another view is that the lack of obvious differentiation of cell types could reflect lack of evolutionary pressure, a result of "relaxed" selection (for non-neurobiology review see Lahti et al., 2009). This is a viable explanation in light of the accumulating evidence that turtles might be sister to archosaurs (discussed extensively in chapter 2). Within this framework, the common ancestor of turtles and archosaurs (or all of the reptiles) might have been able to hear somewhat higher frequencies than modern turtles and therefore had a well-developed auditory system (Gleich et al., 2005). In the case of the turtle auditory system, as the selective pressure for higher best frequency hearing decreased, the precision of organization of the auditory system may have decreased as well.

The data presented here do not give definitive support to a particular hypothesis. We consider it most likely that turtles represent a closer approximation of the ancestral condition. There is no evidence that the common ancestor of the reptiles was an auditory specialist. As some other reptiles are auditory specialists (e.g. barn owls, geckos), a parsimonious explanation is that the ancestral condition was an auditory generalist, possibly only hearing low frequencies as turtles do. However, with the current lack of consensus on the evolutionary position of turtles, the data are difficult to interpret. Future molecular and developmental studies would shed light on these hypotheses.

5 Acknowledgements

The authors thank A. Johny for assistance with tissue processing and neuron reconstruction. We thank C. McCormick and E. Peterson for their use of histological material. We thank J. Chrabaszcz for statistical expertise.

Chapter 4: Development of an Isolated Head In Vivo Physiology Preparation

1 Introduction

Turtles are resistant to anoxia, presumably as an adaptation to hibernation. They have therefore been a favored preparation for isolated brain experiments. These include auditory neurophysiology experiments on hair cells and auditory nerve in the half head preparation (Crawford & Fettiplace, 1981a; 1983; Art & Fettiplace, 1987; Art et al., 1995). The basilar papilla of turtles can also be isolated and recorded from in vitro. This preparation continues to yield insights about the ionic and biophysical underpinnings of hair cell function (Schnee et al., 2005; 2011; 2013).

Turtle isolated brain or isolated brain regions have been used in physiology experiments focused on the cerebellum (Rice & Nicholson, 1990) and a visual cortex preparation that includes the optic nerve and eye (Connors & Kriegstein, 1986; Kriegstein & Connors, 1986; Du et al., 2006). Properties of turtle cortex, which is three-layered, have been studied extensively (Larkum et al., 2008). Experiments have been done in vivo using chronically implanted electrodes (Rutishauser et al., 2013) and in vitro (Du et al., 2006; Rice & Nicholson, 1990). Models of biomechanics of hair cell stereocilia have been derived from isolated turtle basilar papilla preparations (Breneman et al., 2009).

The turtle auditory system has been recorded from in vivo. There is a published experiment on physiological traits of turtle auditory nerve in an intact animal (e.g. Manley, 1971), where Manley showed that turtles have higher thresholds

than other reptiles. including birds. Turtle nerve fibers responded up to 1 kHz, and lowest thresholds were from 100-500 Hz. We initially repeated these experiments, but both surgical and anesthesia issues led us to develop an isolated head preparation that kept the ear intact.

Isolated brain preparations have been developed in a variety of animals, including mammals and many invertebrates. Some of these, like the experiments described in this chapter, leave relevant peripheral structures intact. In mammals, isolated brain preparations are generally maintained by perfusion through the basilar artery with a blood substitute or artificial cerebrospinal fluid (ACSF) (Llinás & Mühlethaler, 1988). In other cases, the isolated brain can be submerged in ACSF. The time over which this this preparation remains viable depends largely on the animal. As mentioned above, turtle preparations are viable for long periods of time, as are many invertebrate preparations.

An isolated turtle brain preparation offers advantages over traditional in vivo and in vitro (slice) preparations. Unlike in vitro preparations, the entirety of the brain's circuitry is preserved. Keeping the ear intact enables use of acoustic instead of electrical stimuli, while an isolated head preparation avoids the difficulties of keeping a turtle sufficiently anesthetized. The half head preparation used by Crawford and Fettiplace (1981) to record from the auditory nerve demonstrated that it was a viable physiological preparation. Therefore, we used the whole head, with a craniotomy to expose the areas of interest. We hypothesized that we would be able to evoke single unit responses in the brain using acoustic stimuli.

2 Method Development

2.1 Anesthesia

All experiments were approved by the University of Maryland Institutional Animal Care and Use Committee (IACUC). In initial experiments, we used Euthasol for anesthesia. These experiments did not yield physiological data. Barbiturates are metabolized slowly (Freudenthal & Carroll, 1974). Therefore following the advice of the campus veterinarian and MacLean et al. (2008), we changed to Propofol, which acts quickly and is metabolized quickly (Short & Bufalari, 1999). This allows for the animal to be anesthetized for rapid decapitation and the brain to recover by the time we started the physiology recording.

2.2 Isolated Head and Surgical Approach

In vivo recordings in turtles present a variety of technical difficulties. Turtles are difficult to anesthetize and keep anesthetized, with a high likelihood of overdose. If the animal is not deeply anesthetized, it can still withdraw its head into its shell. The force of this is enough to detach the post used to control head position during surgery and recording. Since turtle brains are remarkably resistant to anoxia damage (e.g. Hailey et al., 1991; Rodgers-Garlick et al., 2013) we developed the whole head preparation, with a craniotomy to expose the areas of interest. We administered Propofol (5 mg/kg) (MacLean 2008) intravenously through the dorsal sinus. When anesthesia was confirmed by absence of toe pinch and eye blink reflexes, the animal was rapidly decapitated. The splenius capitus (head withdrawal muscle) was removed from the skull. A craniotomy exposed the midbrain and brain stem. The cerebellum

was removed. The head was held in a constant position by gluing a stainless steel head post to the prefrontal bone.

2.3 Temperature

Temperature was an important variable. In the sound-attenuating chamber, temperatures were typically 17-18°C. In standard in vivo experiments in this room, a heating pad controlled by feedback surrounds the animal. This was not possible with an isolated head. The turtles used in our experiments live in a climate-controlled room that rarely falls below 21°C, and is generally at 25°C during the day. Turtles are sensitive to temperature changes (Hailey et al., 1991). Therefore, we utilized a space heater to maintain the temperature of the room between 22-24°C. See Table 4.1 for comparisons between experiments at 18 and 23°C.

2.4 ACSF Testing

We began by using the ACSF recipe used in avian slice preparations (e.g. MacLeod & Carr, 2005). This solution maintained sufficient brain health for dye transport (Chapter 3) but did not appear sufficient for prolonged physiological recordings. We then used a solution developed for an in vitro turtle cerebellum preparation that contained tetramethylammonium chloride (Rice & Nicholson, 1990). This solution yielded a viable preparation for around 1 hour. Another ACSF solution contained 0.005 M imidazole (Rodgers-Garlick et al., 2013). This solution yielded no activity.

The most effective ACSF was comprised of 96.5mM NaCl, 2.6mM KCl, 4.4mM CaCl2, 2.0mM MgCl2, 31.5mM NaCO3, and 10mM dextrose, dissolved in

distilled deionized water and developed for a turtle forebrain preparation (Connors & Kriegstein, 1986). In vivo-like recordings were made from this isolated head preparation. These preparations generally remained responsive for 8- 10 hours. One preparation was responsive after being maintained in oxygenated ACSF in a 4°C refrigerator overnight.

2.5 Oxygenation and Superfusion

Solutions were fully saturated with oxygen. Effects of oxygen are described in detail by Hailey et al. (1991), who also developed an isolated turtle preparation. ACSF was bubbled with 95% O2-5%CO2 gas for 10 minutes before use and again every 2-3 hours. An early version of this preparation involved a small craniotomy such that ACSF covered the brain during recording. The preparation was unstable due to small changes in ACSF level moving the brain. Therefore we set up a slow drip of ACSF that superfused the brain. This was done with IV tubing secured so that the opening of the tube was just rostral to the edge of the craniotomy. A small wick was secured under the tubing and over the edge of the skull into the craniotomy. This prevented electrical artifacts. To aid in superfusion, a second wick was secured at the caudal end of the head so ACSF would flow off and into a container to be re-oxygenated and recycled. These modifications resulted in an in vivo physiological preparation with an intact periphery that remained viable for 12 or more hours.

Case	Units	Temperature (°C)	ACSF
71013	6	18	Avian
71613	7	18	Avian
72313	2	18	Rodgers-Garlick , et al
72613	2	18	Fettiplace & Crawford
8113	8	18	Fettiplace & Crawford
9313	6	18	Fettiplace & Crawford
91713	0	18	Fettiplace & Crawford
10313	1	18	Rice & Nicholson
10813	4	18	Rice & Nicholson
101013	0	18	Rice & Nicholson
101513	16	20	Connors & Kriegstein
103013	12	20	Connors & Kriegstein
103113	7	22	Connors & Kriegstein
121116	8	22	Connors & Kriegstein
121613	16	22	Connors & Kriegstein
12714	12	23	Connors & Kriegstein
2514	30	24	Connors & Kriegstein

Table 4.1: Temperature and ACSF effects on numbers of units recorded.

3 Methods Used for Proof of Concept Data

These experiments provide data from eight adult Red-eared Slider Turtles (*Trachemys scripta elegans*) of both sexes. All animal care and experimental procedures followed procedures approved by the University of Maryland Animal Care And Use Committee. Propofol (5 mg/kg) (MacLean 2008) was administered, and when anesthesia is confirmed by absence of toe pinch and eye blink reflexes, the animal was rapidly decapitated as described above. A craniotomy exposed the midbrain and brain stem. The cerebellum was removed. The head was held in a constant position by gluing a stainless steel head post to the prefrontal bone. IV tubing with a regulator was used to superfuse the exposed brain tissue with oxygenated ACSF.

3.1 Data Collection

Data were obtained with tungsten microelectrodes (F. Haer, Bowdoin ME), with impedances around 20 MΩ. Electrodes were positioned above the acoustic tubercle and advanced remotely in 5-10μm steps. We continuously tested for auditory responses using a variety of monaural and binaural stimuli. Electrodes were coupled to a preamplifier and amplifier system (μA200, Walsh electronics); the amplified signal was high-pass filtered at 300 Hz and fed to an A/D converter (TDT DD1) with subsequent event counter (TDT ET1). Both the analog and the TTL signal were stored and processed by custom-written software (xdphys, Caltech, Pasadena CA).

Recordings were made in a sound-attenuating chamber (IAC, Hannover MD). The chamber was maintained at 22-24°C using a commercial space heater. Closed, custom-made sound systems were placed around the tympanic disk on both ears,

containing commercial miniature earphones and miniature microphones (Knowles EM 3068). The sound systems were sealed against the head using Gold Velvet II ear impression material (All American Mold Laboratories, Oklahoma City, OK), and the sound systems were calibrated individually before the recordings.

Acoustic stimuli (tones and clicks) were digitally generated by the same custom-written software as above, driving a signal-processing system (Tucker Davis Technology, Gainesville, FL). Stimuli were generated separately for the two ears by using a TDT AP2 signal processing board. Both channels were then fed to the earphones via D/A converters (TDT DD1), anti-aliasing filters (TDT FT6-2) and attenuators (TDT PA4). Tone bursts had 100ms duration (including 5ms linear ramps) and were presented at a rate of 5/s. We measured monaural iso-level frequency responses and rate-intensity functions at best frequency for both ipsi- and contralateral stimulation. Condensation clicks had a rectangular form and duration of 2 samples (equivalent to 41.6 μs). The standard click had 0 dB attenuation relative to 85 dB SPL. Interaural time differences (ITD) were tested within ± 1 stimulus period, in steps no larger than 1/10 of the period and stimulus durations of 100msec. Stimulus levels were between 70-85 dB SPL and 10-15 stimulus repetitions were presented at each ITD.

4 Results

We present proof of concept data to support the viability of the isolated head preparation. These data show that we can acquire physiological recordings sufficient to characterize the properties of the turtle brain stem auditory circuit. From 17 animals used (Table 4.1), we used 7 for the data shown in this chapter, giving a total

of 101 units. These data were acquired at 20-24°C using the ACSF recipe from Connors and Kriegstein (1986).

Best frequency was measured for each unit. Some of these normalized responses are shown in Figure 4.1. Best frequencies for single units ranged from 100-400 Hz. The width of the tuning curves varied, and some units have smaller side peaks. Auditory thresholds were measured at best frequency. Most units have a threshold between 60-70 dB SPL (Fig. 4.1). The lowest single unit threshold was 45 dB SPL.

With the isolated head preparation, we were able to record from both first order nuclei and their targets. The majority of isolated units were obtained from recordings from the superficial regions of the acoustic tubercle, and were monaural. Some deeper recordings were binaurally driven. Of these binaural units, most, but not all, were ITD sensitive. These show a range of ITD tuning (Fig. 4.1).

Turtle auditory units phased locked to the auditory stimulus. Phase locking was measured at best frequency (Fig. 4.1). Phase locking vector strength varied from 0.22-0.91; most were above 0.7. We also generated post-stimulus time histograms (Fig. 4.1), and used broadband clicks to measure delays. An example of a binaural unit is shown in Figure 4.1.

5 Discussion

5.1 Optimization

The ACSF formulation, along with temperature control, was key to obtaining viable recordings. The recipe we used was optimized for turtle in vitro recordings. The superfusion rates of oxygenated ACSF were similar to the set-up of many in vitro

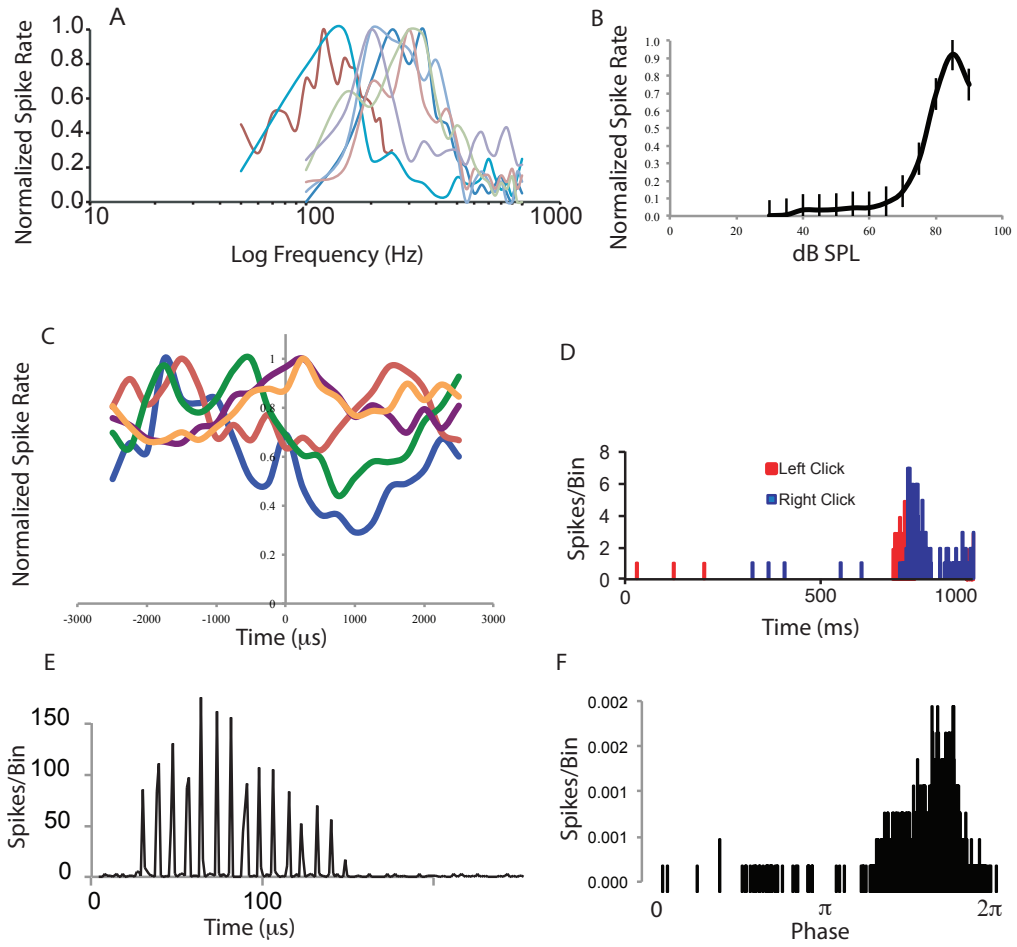

Figure 4.1 Proof of concept data from the isolated head preparation
A. Best frequency curves showing the range of BFs recorded
B. Average thresholds taken at BF from 53 units. Error bars are standard deviation
C. Normalized ITD curves showing the range of ITD sensitivities
D. Example click response in a binaural unit. Binaural units were excitatory-excitatory,
E. Example poststimulus time histogram. PSTH shapes were similar to those described for auditory nerve (Crawford & Fettiplace, 1980, 1983). Bin size is 20 ms
F. Example phase histogram (VS = 0.88). Vector strengths ranged from 0.22-0.91. Bin size is 33 µs

physiology experiments. Keeping the preparation warm yielded a larger number of stable recordings. The minimum temperature at which we obtained stable recordings overlapped with the temperature range at which the animals were housed.

5.2 Best Frequencies

The range of best frequencies recorded are consistent with published audiograms (Christensen-Dalsgaard et al., 2012), but we were concerned that we did not record frequencies above 500 Hz. Auditory Evoked Potential (AEP) audiograms show responses at 1 kHz and lowest thresholds at 500 Hz. Higher frequency units have been recorded by others (Hailey et al., 1991; Manley, 1971). It is possible that higher temperatures will be required, although Hailey et al. used temperatures up to 40 °C (1991) and found no units with a best frequency above 400 Hz. However, turtles hear above 400 Hz (Christensen-Dalsgaard et al., 2012), and Crawford and Fettiplace (1980) recorded two auditory nerve units with best frequencies of 600 Hz. There should, therefore, be neurons with best frequencies higher than we and others have found. This could be an effect of temperature, the type of preparation, or simply being in the low-frequency location.

These recordings complement those from in vivo nerve recordings (Manley, 1971). Manley found auditory nerve units responsive from 50-1000 Hz. Lowest thresholds were from 150-500 Hz. Compared to other reptiles, including birds, turtles had the highest thresholds, except for Leopard lizards (*Gambelia wislizenii*). Manley also showed that relative to other reptiles, turtle auditory nerve fibers tended to have the lowest best frequencies. Finding units tuned to higher frequencies is a primary aim of the further physiological study of the turtle auditory system.

The properties of units we have recorded are similar to those found in auditory nerve and hair cells by Fettiplace, Crawford, Art, Ricci and others. Turtle hair cells have been described physiologically, biophysically, and biochemically. Hair cells are tonotopically organized along the basilar papilla, electrically tuned, and each resonates at its best frequency (Crawford & Fettiplace, 1981a, 1981b). Hair cells and auditory nerve fibers in the turtle have sharp tuning curves up to 600 Hz (Crawford & Fettiplace, 1980; Wu & Fettiplace, 1996). Hair cells rely on a calcium-activated potassium channels for their tuning (Art et al., 1995). To both acoustical and mechanical displacement of hair cells, the auditory nerve responds best below 500 Hz, but does respond to high intensity stimulation (90-100 dB SPL) up 1 kHz (Crawford & Fettiplace, 1983). More experiments in the higher-frequency range of turtle hearing (500-1000 Hz) will prove interesting from stimulus transduction and encoding viewpoints.

5.3 ITD Coding

The most novel result from the development of this preparation emerged from recording from the second order auditory nuclei. We found that the turtle brain encodes a range of ITDs. This will be the focus of future experiments. It should be difficult for the turtle brain to encode a range of ITDs due the interaction between small head size and low frequency hearing. The wavelength of sounds below 1 kHz is much greater than the turtle head size, with wavelengths of 100 Hz in air being about 3.4m, and thus about 70cm in water. Low frequency sounds should therefore be difficult to localize with a small interaural distance. Further investigation of ITD

coding in turtles should reveal the turtles' solution to encoding ITD as well as insight into the evolution of this circuit.

6 Acknowledgements

We acknowledge R. Fettiplace and K. Macleod for technical advice and A. Johny for assistance.

Chapter 5: Discussion, Implications, and Future Directions

One of the major goals of this dissertation is to add to understanding of the evolution of hearing by adding a taxon to this field. Excellent research has been published on the testudine auditory periphery (i.e. hair cells). This dissertation focuses on central processing in the context of evolution. The experiments described here give insight into how binaural hearing evolved.

An advantage of studying the auditory system is that bony elements associated with tympanic hearing (e.g. the otic notch) can be traced through the fossil record (Clack, 1997). Observing middle ear structure across taxa, we are able to form hypotheses about how ear structure affects binaural processing. The fossil record indicates that turtles lost acoustic coupling of the ears at some point in their evolutionary history. This loss must have affected binaural processing. Coupled ears (or pressure difference receiver ears) provide essentially an expansion of the head, yielding a larger range of possible ITDs (Christensen-Dalsgaard & Manley, 2008; Christensen-Dalsgaard et al., 2011), and increased sensitivity to both ITDs and ILDs. A possible selective pressure for the loss of coupled ears might have been testudines becoming secondarily aquatic (Hetherington, 2008). Ears coupled through the mouth would change function drastically as the animal opened and closed its mouth underwater.

Turtles are additionally interesting because they have lower auditory thresholds to underwater sounds, although they also hear in air (Christensen-

Dalsgaard et al., 2012). The exact effects of hearing underwater on central auditory processing are not clear. Moving forward on this question would require comparisons of species from both aquatic and terrestrial environments. Effects of ecological niche on neural processing could be investigated using the turtle auditory system in a fairly direct way. One of the most intriguing questions is what comprises the testudine auditory scene, both aquatically and terrestrially. Extensive investigation, beginning with careful observation, is merited for this question.

Although the evolutionary position of testudines is not yet resolved, close study of testudine anatomy and physiology can provide insight. I agree with the hypotheses from molecular evolution studies that testudines share their most recent common ancestor with the archosaurs (Hedges & Poling, 1999; Iwabe, 2005; Shen et al., 2011; Chiari et al., 2012; Crawford et al., 2012), and testudines may reflect the ancestral condition for the archosaur clade. Comparing turtles with avian auditory specialists could therefore aid understanding of the auditory circuit. Close examination of neurochemistry and development would enhance this understanding.

In mammals, birds and lizards, the tonotopically-arranged basilar papilla (or cochlea) is mapped tonotopically in the brain. There are varying degrees of precision in these maps. Experiments are in progress to determine how tonotopy is mapped in the turtle brain stem. Insight will be gained from these experiments on how an animal that is not an auditory specialist maps tonotopy as well as how the mapping compares in closely related animals. The axes of the maps may give insight into developmental processes.

Although we do not yet know how the NM-NL circuit functions in turtles, NA, NM and NL are similarly organized in turtles, birds, crocodilians, and geckos. The turtle NM is smaller and less well developed than in birds and crocodilians, and NM's target, NL, was also smaller, but all NL neurons were bitufted with segregated ipsi- and contralateral inputs from NM (Young and Rubel, 1986; MacLeod et al., 2006; Tang et al., 2011; for reviews see Grothe et al., 2005; Carr et al., 2009). Given these similarities, I hypothesize that NL appeared in the shared ancestor of the archosaurs and lepidosaurs. Further physiological investigations may support a role for NL in ancestral reptiles.

The experiments described in this dissertation are interesting from the perspectives of evolution and neural processing. Further experiments may reveal how evolution and environment interact to shape both neuroanatomy and neural processing. The physiological preparation developed should reveal the function of auditory brainstem circuits. The ITD range I recorded is of great interest. It shows that turtles, which should have great difficulty with ITD detection, appear to have neural compensations that are good enough for sound localization. The ITD range should be small because of the head size. Possible solutions include behavioral adaptations (e.g. head movements) and changes in myelination of the NM axons. A small range may be sufficient for a testudine auditory scene. All of these factors result in auditory processing in testudines being a fruitful topic for further investigation.

Bibliography

Adolphs, R. (1993). Bilateral inhibition generates neuronal responses tuned to interaural level differences in the auditory brainstem of the barn owl. Journal of Neuroscience, 13(9), 3647–3668.

Adrian E, Craik K, Sturdy R (1938) The electrical response of the auditory mechanism in cold blooded vertebrates. Proc Roy Soc B 125, 435–455.

Ariëns Kappers, C. U., Huber, G. C., & Crosby, E. C. (1936). The comparative anatomy of the nervous system of vertebrates, including man. New York: Macmillan.

Art, J. J., & Fettiplace, R. (1987). Variation of membrane properties in hair cells isolated from the turtle cochlea. J Physiol, 385, 207–242.

Art, J. J., Wu, Y.-C., & Fettiplace, R. (1995). The calcium-activated potassium channels of turtle hair cells. J Gen Physiol, 105, 49–72.

Ashida, G., & Carr, C. E. (2011). Sound localization: Jeffress and beyond. Current Opinion in Neurobiology, 21(5), 745–751

Barbas-Henry, H. A., & Lohman, A. H. (1988). Primary projections and efferent cells of the VIIIth cranial nerve in the monitor lizard, *Varanus exanthematicus*. Journal of Comparative Neurology, 277(2), 234–249.

Bartol, S. M., Musick, J. A., & Lendhardt, M. L. (1999). Auditory evoked potentials of the loggerhead sea turtle (Caretta caretta). Copeia, 1999(3), 836–840.

Belekhova, M. G., Zharskaja,V.D., Khachunts, A. S.,Gaidanenko,G. V.,&Tumanova,N. L. (1985). Connections of the mesencephalic, thalamic and

telencephalic auditory centers in turtles: Somestructural bases for audiosomatic interrelations. Journal fu¨r Hirnforschung, 26(2), 127–152.

Belekhova, M. G., Kenigfest-Rio, N. B., Vesslkin, N. P., Rio, J.-P., Reperant, J., & Ward,R. (2002). Evolutionary significance of different neurochemical organisation of the internaland external regions of auditory centres in the reptilian brain: An immunocytochemical andreduced NADPH-diaphorase histochemical study in turtles. Brain Research, 925, 100–106.

Belekhova, M. G., Chudinova, T. V., Kenigfest, N. B., & Krasnoshchekova, E. I. (2008).Distribution of metabolic activity (cytochrome oxidase) and immunoreactivity to calcium binding proteins in the turtle brainstem auditory nuclei. Journal of Evolutionary Biochemistry and Physiology, 44(3), 354–364.

Belekhova, M. G., Chudinova, T. V., Repe´rant, J., Ward, R., Jay, B., Vesselkin, N. P., & Kenigfest, N. B. (2010). Core-and-belt organisation of the mesencephalic and forebrain auditory centres in turtles: Expression of calcium-binding proteins and metabolic activity. Brain Research, 1345, 84–102.

Bierman, H. S., Carr, C. E., Brandt, C., Young, B. A., & Christensen-Dalsgaard, J. (2011). Evidence for low-frequency sound localization in the American alligator (Alligator mississippiensis). Neuroscience Meeting Planner. Washington, DC: Society for Neuroscience.

Breneman, K. D., Highstein, S. M., Boyle, R. D., & Rabbitt, R. D. (2009). The Passive Cable Properties of Hair Cell Stereocilia and Their Contribution to

Somatic Capacitance Measurements. Biophysical Journal, 96(1), 1–8. doi:10.1529/biophysj.108.137356

Brinkman DB (2005) A vertebrate assemblage from the marine shales of the Lethbridge Coal Zone. In P. J. Currie and E. B. Koppelhus (eds.) Dinosaur Provincial Park, A spectacular ancient ecosystem revealed. Indiana University Press, Bloomington and Indianapolis, Indiana.

Browner, R. H., & Marbey, D. (1988). The nucleus magnocellularis in the red-eared turtle, Chrysemys scripta elegans: Eighth nerve endings and neuronal types. Hear Res, 33, 257–272.

Burger, R. M., & Rubel, E. W (2008). Encoding of interaural timing for binaural hearing. In A. I. Basbaum, G. M. Shepherd, & G. Westheimer (Eds.), The senses: A comprehensive reference (Vol. 3, pp. 613–630). San Diego: Academic Press.

Calford, M. B., & Piddington, R. B. (1988). Avian interaural canal enhances interaural delay. Journal of Comparative Physiology A, 162, 503–510.

Campbell HW, Evans WE (1972) Observation on the vocal behavior of chelonians. Herpetologica 28, 277–280.

Campbell HW, Evans WE (1967) Sound production in two species of tortoises. Herpetologica 23, 204–209.

Capranica, R. R. (1966). Vocal response of the bullfrog to natural and synthetic mating Calls. Journal of the Acoustical Society of America, 40, 1131–1139.

Carr A F (1969) Handbook of turtles; the turtles of the United States, Canada, and Baja California. Ithaca, N.Y.: Comstock Pub.

Carr, C. E. (1993). Processing of temporal information in the brain. Annual Review of Neuroscience, 16, 223–243.

Carr, C. E., & Konishi, M. (1990). A circuit for detection of interaural time differences in the brain stem of the barn owl. Journal of Neuroscience, 10(10), 3227–3246.

Carr, C. E., & Boudreau, R. E. (1991). Central projections of auditory nerve fibers in the barn owl. Journal of Comparative Neurology, 314, 306–318.

Carr, C. E., & Code, R. A. (2000). Anatomy and physiology of the central auditory system of birds and reptiles. In A. N. Popper, R. R. Fay, & R. J. Dooling (Eds.), Comparative hearing: Birds and reptiles. New York: Springer Science+Business Media.

Carr, C. E., & Soares, D. (2002). Evolutionary convergence and the shared computational principles in the auditory system. Brain, Behavior and Evolution, 59, 294–311.

Carr, C. E., & Koppl, C. (2004). Coding interaural time differences at low best frequencies in the barn owl. Journal of Physiology, Paris, 98(1–3), 99–112.

Carr, C. E., & Edds-Walton, P. (2008). Vertebrate auditory pathways. In R. Hoy, P. Dallos, &D. Oertel (Eds.), Handbook of the senses, Vol. 1: Audition. Oxford: Elsevier.

Carr, C. E., Fujita, I., & Konishi, M. (1989). Distribution of GABAergic neurons and terminals in the auditory system of the barn owl. Journal of Comparative Neurology, 286, 190–207.

Carr, C. E., Soares, D., Smolders, J., & Simon, J. Z. (2009). Detection of interaural time differences in the alligator. Journal of Neuroscience, 29(25), 7978–7990.

Chiari, Y., Cahais, V., Galtier, N., & Delsuc, F. (2012). Phylogenomic analyses support the position of turtles as the sister group of birds and crocodiles (Archosauria). BMC Biology, 10(1), 65–79.

Christensen, C. B., Christensen-Dalsgaard, J., Brandt, C., & Madsen, P. T. (2011). Hearing with an atympanic ear: Good vibration and poor sound-pressure detection in the royal python, *Python regius*. Journal of Experimental Biology, 215(2), 331–342.

Christensen-Dalsgaard, J. (2005). Directional hearing in nonmammalian tetrapods. In R. R. Fay & A. N. Popper (Eds.), Sound source localization. (pp. 67–123). New York: Springer Science +Business Media.

Christensen-Dalsgaard, J. (2009). Amphibian bioacoustics. In S. Kuwano & M. Vorlander (Eds.), Handbook of signal processing in acoustics (pp. 1861–1885). New York: Springer.

Christensen-Dalsgaard, J. (2011). Vertebrate pressure-gradient receivers. Hearing Research, 273 (1–2), 37–45.

Christensen-Dalsgaard J, Elepfandt A (1995) Biophysics of underwater hearing in the clawed frog. J comp Physiol A 176, 1–8.

Christensen-Dalsgaard, J., & Kanneworff, M. (2005). Binaural interaction in the frog dorsal medullary nucleus. Brain Research Bulletin, 66(4–6), 522–525.

Christensen-Dalsgaard, J., & Manley, G. A. (2005). Directionality of the lizard ear. Journal of Experimental Biology, 208(6), 1209–1217.

Christensen-Dalsgaard, J., & Carr, C. E. (2008). Evolution of a sensory novelty: Tympanic ears and the associated neural processing. Brain Research Bulletin, 75(2–4), 365–370.

Christensen-Dalsgaard, J., & Manley, G. A. (2008). Acoustical coupling of lizard eardrums. Journal of the Association for Research in Otolaryngology, 9(4), 407–416.

Christensen-Dalsgaard, J., Tang, Y., & Carr, C. E. (2011). Binaural processing by the gecko auditory periphery. Journal of Neurophysiology, 105(5), 1992–2004.

Christensen-Dalsgaard, J., Brandt, C., Willis, K. L., Christensen, C. B., Ketten, D., Edds-Walton, P., Fay, R. R., Madsen, P. T., & Carr, C. E. (2012). Specialization for underwater hearing by the tympanic middle ear of the turtle, Trachemys scripta elegans. Proceedings of the Royal Society of London B: Biological Sciences, 279(1739), 2816–2824.

Clack, J. A. (1997). The evolution of tetrapod ears and the fossil record. Brain, Behavior and Evolution, 50, 198–212.

Clack, J. A. (2002). Gaining ground: The origin and evolution of tetrapods. Bloomington: Indiana University Press.

Clack, J. A. (2002). Patterns and processes in the early evolution of the tetrapod ear. Journal of Neurobiology, 53(2), 251–264. doi:10.1002/neu.10129

Clack, J. A., & Allin, E. (2004). The evolution of single-and multiple-ossicle ears in fishes and tetrapods. In G. A. Manley, A. N. Popper, & R. R. Ray (Eds.), Evolution of the vertebrate auditory system (pp. 128–163). New York: Springer Science+Business Media.

Coles, R. B., & Guppy, A. (1988). Directional hearing in the barn owl (Tyto alba). Journal of Comparative Physiology A, 163(1), 117–133.

Connors, B. W., & Kriegstein, A. R. (1986). Cellular physiology of the turtle visual cortex: distinctive properties of pyramidal and stellate neurons. J Neurosci, 6(1), 164–177.

Covey, E., & Carr, C. E. (2004). The auditory midbrain in bats and birds. In J. A. Winer & C. E. Schreiner (Eds.), The inferior colliculus. New York: Springer Science+Business Media.

Cramer, K. S., Fraser, S. E., & Rubel, E. W (2000). Embryonic origins of auditory brain-stem nuclei in the chick hindbrain. Developmental Biology, 224(2), 138–151.

Crawford, A. C., & Fettiplace, R. (1980). The frequency selectivity of auditory nerve fibres and hair cells in the cochlea of the turtle. Journal of Physiology, 306, 79–125.

Crawford, A. C., & Fettiplace, R. (1981a). An electrical tuning mechanism in turtle cochlear hair cells. J Physiol, 312, 377–412.

Crawford, A. C., & Fettiplace, R. (1981b). Non-linearities in the responses of turtle hair cells. J Physiol, 315, 317–338.

Crawford, A. C., & Fettiplace, R. (1983). Auditory nerve responses to imposed displacements of the turtle basilar membrane. Hear Res, 12, 199–208.

Crawford, N. G., Faircloth, B. C., McCormack, J. E., Brumfield, R. T., Winker, K., & Glenn, T. C. (2012). More than 1000 ultraconserved elements provide

evidence that turtles are the sister group of archosaurs. Biology Letters, 8(1), 1–4.

Dı´az, C., Yanes, C., Trujillo-Ceno´z, C. M., & Puelles, L. (2000). Cytoarchitectonic subdivisions in the subtectal midbrain of the lizard Gallotia galloti. Journal of Neurocytology, 29(8), 569–593.

Drakontides, A. B., & Browner, R. H. (1986). Ultrastructural features of the ventromedial region of the laminar nucleus in the red-eared turtle (Chrysemys scripta elegans). The Journal of Comparative Neurology, 248(4), 555–572. doi:10.1002/cne.902480408

Du, X., Ghosh, B. K., & Ulinski, P. (2006). Encoding of Motion Targets by Waves in Turtle Visual Cortex. IEEE Transactions on Biomedical Engineering, 53(8), 1688–1695. doi:10.1109/TBME.2006.877796

Du¨ring, M., Karduck, A., & Richter, H.-G. (1974). The fine structure of the inner ear in Caiman crocodilus. Anatomy and Embryology, 145(1), 41–65.

Eatock, R. A., Manley, G. A., & Pawson, L. (1981). Auditory nerve fibre activity in the tokay gecko. Journal of Comparative Physiology A, 142(2), 203–218.

Euston, D. R., & Takahashi, T. T. (2002). From spectrum to space: The contribution of level difference cues to spatial receptive fields in the barn owl inferior colliculus. Journal of Neuroscience, 22(1), 284–293.

Evans HM (1925) A Contribution to the Anatomy and Physiology of the Air- Bladder and Weberian Ossicles in Cyprinidae. Proc Roy Soc B 97, 545–576.

Foster, R. E., & Hall, W. C. (1978). The organization of central auditory pathways in a reptile, *Iguana iguana*. Journal of Comparative Neurology, 178(4), 783–831.

Frazier J, Peters G (1981) The call of the Aldabra tortoise (*Geochelone gigantea*) (Reptilia, Testudinidae). Amphibia-Reptilia 2, 1–17.

Freudenthal, R. I., & Carroll, F. I. (1974). Metabolism of certain commonly used barbiturates. Drug Metabolism Reviews, 2(1), 265–278.

Friedel, P., Young, B., & van Hemmen, J. (2008). Auditory localization of ground-borne vibrations in snakes. Physical Review Letters, 100(4), 048701.

Funabiki, K., Koyano, K., & Ohmori, H. (1998). The role of GABAergic inputs for coincidence detection in the neurones of nucleus laminaris of the chick. Journal of Physiology, 508(3), 851–869.

Gaffney ES (1983) Skull Morphology of the Oldest Turtles: A Preliminary Description of *Proganochelys quenstedti*. J Vert Paleontol 3, 25–28.

Gaffney ES (1972) An Illustrated Glossary of Turtle Skull Nomenclature. American Museum Novitates, 1–33.

Gans, E., Willis, K. L., Bierman, H. S., & Carr, C. E. (2012). The interaural canal of the barn owl, Tyto alba. Society for Integrative and Comparative Biology Meeting Planner. Charleston, SC:

Giles JC, Davis JA, McCauley RD, Kuchling G (2009) Voice of the turtle: The underwater acoustic repertoire of the long-necked freshwater turtle, *Chelodina oblonga*. J. Acoust. Soc. Am. 126, 434–443.

Glatt, A. F. (1975a). Vergleichend morphologische Untersuchungen am akustischen System einiger ausgewahlter Reptilien. A. Caiman crocodilus. Revue Suisse De Zoologie: Annales De La Socie´te´ Zoologique Suisse Et Du Museum D'histoire Naturelle De Geneve, 82(2), 257–281.

Glatt, A. F. (1975b). Vergleichend morphologische Untersuchungen am akustischen System einiger ausgewa¨hlter Reptilien. B: Sauria, Testudines. Revue Suisse De Zoologie Annales De La Socie´te´ Zoologique Suisse Et Du Museum D'histoire Naturelle De Geneve, 82, 469–494.

Gleich, O., Dooling, R. J., & Manley, G. A. (2005). Audiogram, body mass, and basilar papilla length: Correlations in birds and predictions for extinct archosaurs. Naturwissenschaften, 92 (12), 595–598.

Grothe, B. (2003). Sensory systems: New roles for synaptic inhibition in sound localization. Nature Reviews Neuroscience, 4(7), 540–550.

Grothe, B., Carr, C. E., Casseday, J. H., Fritzsch, B., & Köppl, C. (2004). The evolution of central pathways and their neural processing patterns. In G. A. Manley, A. N. Popper, & R. R. Fay (Eds.), Evolution of the vertebrate auditory system. New York: Springer Science+Business Media.

Grothe, B., Pecka, M., & McAlpine, D. (2010). Mechanisms of sound localization in mammals. Physiological Reviews, 90(3), 983–1012.

Guillon JM, Guery L, Hulin V, Girondot M (2012) A large phylogeny of turtles (Testudines) using molecular data. Contributions to Zoology 81, 147–158.

Hailey, A., Rosenberg, M. E., & Pullen, A. H. (1991). An in virto brainstem preparation preserving peripheral auditory function. J Neurosci Meth, 39, 217–223.

Hartline, P. (1971a). Physiological basis for detection of sound and vibration in snakes. Journal of Experimental Biology, 54, 349–371.

Hartline, P. (1971b). Mid-brain responses of the auditory and somatic vibration systems in snakes. Journal of Experimental Biology, 54, 373–390.

Hartline, P., & Campbell, H. (1969). Auditory and vibratory responses in the midbrains of snakes. Science, 193(3872), 1221–1223.

Hedges, S. B., & Poling, L. L. (1999). A molecular phylogeny of reptiles. Science, 283(5404), 998–1001.

Hetherington, T. (2008). Comparative anatomy and function of hearing in aquatic amphibians, reptiles, and birds. In J. G. M. Thewissen & S. Nummela (Eds.), Sensory evolution on the threshold: Adaptations in secondarily aquatic vertebrates. Berkeley: University of California Press.

Higgs, D. M., Brittan-Powell, E. F., Soares, D., Souza, M. J., Carr, C. E., Dooling, R. J., & Popper, A. N. (2002). Amphibious auditory responses of the American alligator (*Alligator mississipiensis*). Journal of Comparative Physiology A, 188(3), 217–223.

Hill, K. G., Lewis, D. B., Hutchings, M. E., & Coles, R. B. (1980). Directional hearing in the Japanese quail (Coturnix coturnix japonica). Journal of Experimental Biology, 86, 135–151.

Holmes, G. M. (1903). On the comparative anatomy of the nervus acusticus. Transactions of the Royal Irish Academy, 32, 101–144.

Hunt, R. H., & Watanabe, M. E. (1982). Observations on maternal behavior of the American alligator, *Alligator mississippiensis*. Journal of Herpetology, 16(3), 235–239.

Hyson, R. L. (2005). The analysis of interaural time differences in the chick brain stem. Physiology & Behavior, 86(3), 297–305.

Iwabe N (2005) Sister Group Relationship of Turtles to the Bird-Crocodilian Clade Revealed by Nuclear DNA-Coded Proteins. Molecular Biology and Evolution 22, 810–813.

Jaslow, A. P., Hetherington, T. E., & Lombard, R. E. (1988). Structure and function of the amphibian middle ear. In B. Fritzsch, M. J. Ryan, W. Wilczynski, T. E. Hetherington, & W. Walkeoviak (Eds.), The evolution of the amphibian auditory system (pp. 69–92). New York: John Wiley & Sons.

Jeffress, L. A. (1947). A place theory of sound localization. Journal of Comparative and Physiological Psychology, 41(1), 35–39.

Joris, P. X., Smith, P. H., & Yin, T. C. T. (1998). Coincidence detection in the auditory system: 50 Years after Jeffress. Neuron, 21, 1235–1238.

Kennedy, M. C. (1974). Auditory multiple-unit activity in the midbrain of the Tokay gecko (*Gekko gecko*, L.). Brain, Behavior and Evolution, 10(1–3), 257–264.

Kennedy, M. C., & Browner, R. H. (1981). The torus semicircularis in a gekkonid lizard. Journal of Morphology, 169(3), 259–274.

Ketten DR, Merigo C, Chiddick E, Krum H (1999) Acoustic fatheads: Parallel evolution of underwater sound reception mechanisms in dolphins, turtles, and sea birds. In. Acoustical Society of America Annual Meeting.

Klump, G. M. (2000). Sound localization in birds. In R. J. Dooling, R. R. Fay, & A. N. Popper (Eds.), Comparative hearing: Birds and reptiles (pp. 249–307). New York: Springer Science+Business Media.

Konishi, M. (1970). Comparative neurophysiological studies of hearing and vocalizations in songbirds. Zeitschrift fu¨r vergleichende Physiologie, 66, 257–272.

Köppl, C. (1994). Auditory nerve terminals in the cochlear nucleus magnocellularis: Differences between low and high frequencies. Journal of Comparative Neurology, 339, 438–446.

Köppl, C. (1997). Frequency tuning and spontaneous activity on the auditory nerve and cochlear nucleus magnocelluaris of the barn owl Tyto alba. Journal of Neurophysiology, 77, 364–377.

Köppl, C. (2009). Evolution of sound localisation in land vertebrates. Current Biology, 19(15), R635–R639.

Köppl, C., & Carr, C. E. (1997). Low-frequency pathway in the barn owl's auditory brainstem. Journal of Comparative Neurology, 378, 265–282.

Köppl, C., & Carr, C. E. (2008). Maps of interaural time difference in the chicken's brainstem nucleus laminaris. Biological Cybernetics, 98(6), 541–559.

Kriegstein, A. R., & Connors, B. W. (1986). Cellular physiology of the turtle visual cortex: synaptic properties and intrinsic circuitry. J Neurosci, 6(1), 178–191.

Kruskal, J. B. (1964) Nonmetric multidimensional scaling: a numerical method. Psychometrika, 29, 115-129.

Krützfeldt, N. O. E., Logerot, P., Kubke, M. F., & Wild, J. M. (2010). Connections of the auditory brainstem in a songbird, Taeniopygia guttata.II. Projections of nucleus angularis and nucleus laminaris to the superior olive and lateral lemniscal nuclei. Journal of Comparative Neurology, 518(11), 2135–2148.

Lahti, D. C., Johnson, N. A., Ajie, B. C., Otto, S. P., Hendry, A. P., Blumstein, D. T., et al. (2009). Relaxed selection in the wild. Trends in Ecology & Evolution, 24(9), 487–496.

Larkum, M. E., Watanabe, S., Lasser-Ross, N., Rhodes, P., & Ross, W. N. (2008). Dendritic Properties of Turtle Pyramidal Neurons. Journal of Neurophysiology, 99(2), 683–694. doi:10.1152/jn.01076.2007

Larsen, O. N., Dooling, R. J., & Michelsen, A. (2006). The role of pressure difference reception in the directional hearing of budgerigars (Melopsittacus undulatus). Journal of Comparative Physiology A, 192(10), 1063–1072.

Leake, P. A. (1974). Central projections of the statoacoustic nerve in *Caiman crocodilus*. Brain, Behavior and Evolution, 10(1–3), 170–196.

Lee MSY (2001) Molecules, morphology, and the monophyly of diapsid reptiles. Contributions to Zoology 70, 1–22.

Lesica, N. A., Lingner, A., & Grothe, B. (2010). Population coding of interaural time differences in gerbils and barn owls. Journal of Neuroscience, 30(35), 11696–11702.

Li C, Wu XC, Rieppel O, Wang LT, Zhao LJ (2008) An ancestral turtle from the Late Triassic of southwestern China. Nature 456, 497–501

Llinás, R., & Mühlethaler, M. (1988). Electrophysiology of guinea-pig cerebellar nuclear cells in the in vitro brain stem-cerebellar preparation. The Journal of Physiology, 404(1), 241–258.

Lombard RE, Fay RR, Werner YL (1981) Underwater hearing in the frog, *Rana catesbeiana*. J. Exp. Biol 1981, 57–71.

Lu, B., Yang, W., Dai, Q., & Fu, J. (2013). Using Genes as Characters and a Parsimony Analysis to Explore the Phylogenetic Position of Turtles. PLoS ONE, 8(11), e79348. doi:10.1371/journal.pone.0079348.s002

Lyson, T. R., Bever, G. S., Bhullar, B. A. S., Joyce, W. G., & Gauthier, J. A. (2010). Transitional fossils and the origin of turtles. Biology Letters, 6(6), 830–833.

MacLean, R. A., Harms, C. A., & Braun-McNeill, J. (2008). Propofol anesthesia in loggerhead (*Caretta caretta*) sea turtles. Journal of wildlife diseases, 44(1), 143-150.

MacLeod, K. M., & Carr, C. E. (2005). Synaptic Physiology in the Cochlear Nucleus Angularis of the Chick. Journal of Neurophysiology, 93(5), 2520–2529. doi:10.1152/jn.00898.2004

Manley, G. (1970a). Comparative studies of auditory physiology in reptiles. Zeitschrift fu¨r vergleichende Physiologie, 363–381.

Manley, G. A. (1970b). Frequency sensitivity of auditory neurons in the Caiman cochlear nucleus. Zeitschrift fu¨r vergleichende Physiologie, 66, 251–256.

Manley, G. A. (1971). Some aspects of the evolution of hearing in vertebrates. Nature, 230, 506–509.

Manley, G. A. (1974). Activity patterns of neurons in the peripheral auditory system of some reptiles. Brain, Behavior and Evolution, 10(1–3), 244–256.

Manley, G. A. (1981). A review of the auditory physiology of reptiles. Progress in Sensory Physiology, 2, 49–134.

Manley, G. A. (2000). Cochlear mechanisms from a phylogenetic viewpoint. Proceedings of the National Academy of Sciences of the USA, 97(22), 11736–11743.

Manley, G. A. (2002). Evolution of structure and function of the hearing organ of lizards. Journal of Neurobiology, 53(2), 202–211.

Manley, G. A. (2010). An evolutionary perspective on middle ears. Hearing Research, 263, 3–8.

Manley, G. A., & Köppl, C. (1998). Phylogenetic development of the cochlea and its innervation. Current Opinion in Neurobiology, 8(4), 468–474.

Mannen H, Li SSL (1999) Molecular evidence for a clade of turtles. Molecular Phylogenetics and Evolution 13, 144–148.

Marbey, D., & Browner, R. H. (1985). The reconnection of auditory posterior root fibers in the red-eared turtle, Chrysemys scripta elegans. Hearing Research, 1–4.

Marin, F., & Puelles, L. (1995). Morphological fate of rhombomeres in quail/chick chimeras: A segmental analysis of hindbrain nuclei. European Journal of Neuroscience, 7, 1714–1738.

Mason M, Wang M, Narins PM (2009) Structure and function of the middle ear apparatus of the aquatic frog, *Xenopus laevis*. Proc Inst Acoust 31, 13–21.

McAlpine, D., Jiang, D., & Palmer, A. R. (2001). A neural code for low-frequency sound localization in mammals. Nature Neuroscience, 4(4), 396–401.

McCormick, C. A. (1999). Anatomy of central auditory pathways in fish and amphibians. In A. N.Popper & R. R. Fay (Eds.), Comparative hearing: Fish and amphibians (pp. 155–217). New York: Springer-Verlag.

Miller, M. R. (1980). The cochlear nuclei of snakes. Journal of Comparative Neurology, 192(4), 717–7736.

Miller, M. R., & Kasahara, M. (1979). The cochlear nuclei of some turtles. Journal of Comparative Neurology, 185, 221–236.

Moiseff, A., & Konishi, M. (1981). The owl's interaural pathway is not involved in sound localization. Journal of Comparative Physiology A, 144, 299–304.

Moss, C. F., & Carr, C. E. (2012). Comparative audtion. In M. Gallagher & R. J. Nelson (Eds.), Handbook of psychology (pp. 115–156). Hoboken: John Wiley & Sons.

Northcutt, R. G., & Kaas, J. H. (1995). The emergence and evolution of mammalian neocortex. Trends in Neurosciences, 18(9), 373–379.

Myers P, Espinosa R, Parr CS, Jones T, Hammond GS, et al. (2012) The Animal Diversity Web (online). Available: http://animaldiversity.org.

Overholt, E. M., Rubel, E. W., & Hyson, R. L. (1992). A circuit for coding interaural time differences in the chick brainstem. Journal of Neuroscience, 12(5), 1698–1708.

Passek, K. M., & Gillingham, J. C. (1999). Absence of kin discrimination in hatchling American alligators, *Alligator mississippiensis.* Copeia, 1999(3), 831–835.

Patterson, W. (1966). Hearing in the turtle. Journal of Auditory Research, 6, 453–464.

Pecka, M., Brand, A., Behrend, O., & Grothe, B. (2008). Interaural time difference processing in the mammalian medial superior olive: The role of glycinergic inhibition. Journal of Neuroscience, 28(27), 6914–6925.

Pen˜a, J. L., Viete, S., Funabiki, K., Saberi, K., & Konishi, M. (2001). Cochlear and neural delays for coincidence detection in owls. Journal of Neuroscience, 21(23), 9455–9459.

Pin˜ eiro G, Ferigolo J, Ramos A, Laurin M (2012) Cranial morphology of the Early Permian mesosaurid Mesosaurus tenuidens and the evolution of the lower temporal fenestration reassessed. Comptes rendus - Palevol 11, 379–391.

Plassmann W, Kadel M (1991) Low-frequency selectivity in a gerbilline Rodent, *Pachyurmys dupras*. Brain Behav Evol 38, 115–126.

Polgar G, Malavasi S, Cipolato G, Georgalas V, Clack JA, et al. (2011) Acoustic Communication at the Water's Edge: Evolutionary Insights from a Mudskipper. PLoS ONE 6, e21434.

Popper, A. N., & Fay, R. R. (2011). Rethinking sound detection by fishes. Hearing Research, 273 (1–2), 25–36.

Pritz, M. B. (1974). Ascending connections of a thalamic auditory area in a crocodile, *Caiman crocodilus*. Journal of Comparative Neurology, 153(2), 199–213.

Ravicz ME, Rosowski JJ (1997) Sound-power collection by the auditory periphery of the Mongolian gerbil *Meriones uguiculatus*: III. Effect of variations in middle-ear volume. J Acoust Soc Amer 101, 2135–2147.

Rice, M. E., & Nicholson, C. (1990). Glutamate-and aspartate-induced extracellular potassium and calcium shifts and their relation to those of kainate, quisqualate

and n-methyl-d-aspartate in the isolated turtle cerebellum. Neuroscience, 38(2), 295–310.

Ridgway, S. H., Wever, E. G., McCormick, J. G., Palin, J., & Anderson, J. H. (1969). Hearing in the giant sea turtle, Chelonia mydas. Proceedings of the National Academy of Sciences of the USA, 64, 884–890.

Rieppel O, deBraga M (1996) Turtles as diapsid reptiles. Nature 384, 453–455.

Rieppel O, Reisz RR (1999) The Origin and Early Evolution of Turtles. Annu Rev Ecol Syst 30, 1–22.

Rodgers-Garlick, C. I., Hogg, D. W., & Buck, L. T. (2013). Oxygen-sensitive reduction in Ca2+-activated K+ channel open probability in turtle cerebrocortex. Neuroscience, 237(C), 243–254. doi:10.1016/j.neuroscience.2013.01.046

Rutishauser, U., Kotowicz, A., & Laurent, G. (2013). A method for closed-loop presentation of sensory stimuli conditional on the internal brain-state of awake animals. Journal of Neuroscience Methods, 215(1), 139–155. doi:10.1016/j.jneumeth.2013.02.020

Ryugo, D. K., & Parks, T. N. (2003). Primary innervation of the avian and mammalian cochlear nucleus. Brain Research Bulletin, 60(5–6), 435–456.

Schnee, M. E., Castellano-Munoz, M., & Ricci, A. J. (2013). Response properties from turtle auditory hair cell afferent fibers suggest spike generation is driven by synchronized release both between and within synapses. Journal of Neurophysiology, 110(1), 204–220. doi:10.1152/jn.00121.2013

Schnee, M. E., Lawton, D. M., Furness, D. N., Benke, T. A., & Ricci, A. J. (2005). Auditory Hair Cell-Afferent Fiber Synapses Are Specialized to Operate at Their Best Frequencies. Neuron, 47(2), 243–254. doi:10.1016/j.neuron.2005.06.004

Schnee, M. E., Santos-Sacchi, J., Castellano-Muñoz, M., Kong, J.-H., & Ricci, A. J. (2011). Calcium-Dependent Synaptic Vesicle Trafficking Underlies Indefatigable Release at the Hair Cell Afferent Fiber Synapse. Neuron, 70(2), 326–338. doi:10.1016/j.neuron.2011.01.031

Schnupp, J. W. H., & Carr, C. E. (2009). On hearing with more than one ear: Lessons from evolution. Nature Neuroscience, 12(6), 692–697.

Shen, X. X., Liang, D., Wen, J. Z., & Zhang, P. (2011). Multiple genome alignments facilitate development of NPCL markers: A case study of tetrapod phylogeny focusing on the position of turtles. Molecular Biology and Evolution, 28(12), 3237–3252.

Short, C. E., & Bufalari, A. (1999). Propofol anesthesia. The Veterinary Clinics of North America. Small Animal Practice, 29(3), 747–778.

Smolders, J. W., & Klinke, R. (1986). Synchronized responses of primary auditory fibre populations in *Caiman crocodilus* (L.) to single tones and clicks. Hearing Research, 24(2), 89–103.

Sneary, M. (1988). Auditory receptor of the red-eared turtle: II. Afferent and efferent synapses and innervation patterns. Journal of Comparative Neurology, 276, 588–606.

Soares, D., & Carr, C. E. (2001). The cytoarchitecture of the nucleus angularis of the barn owl (Tyto alba). J Compar Neurol, 429, 192–205.

Stecker, G. C., Harrington, I. A., & Middlebrooks, J. C. (2005). Location coding by opponent neural populations in the auditory cortex. Public Library of Science Biology, 3(3), e78.

Szpir, M. R., Sento, S., & Ryugo, D. K. (1990). Central projections of cochlear nerve fibers in the alligator lizard. Journal of Comparative Neurology, 295(4), 530–547.

Szpir, M. R., Wright, D. D., & Ryugo, D. K. (1995). Neuronal organization of the cochlear nuclei in alligator lizards: A light and electron microscope investigation. Journal of Comparative Neurology, 357, 217–241.

Takahashi, T. T. (1989). Construction of an auditory space map. Annals of the New York Academy of Sciences, 563, 101–113.

Takahashi, T. T., & Konishi, M. (1988a). Projections of the cochlear nuclei and nucleus laminaris to the inferior colliculus of the barn owl. Journal of Comparative Neurology, 274(2), 190–211.

Takahashi, T. T., & Konishi, M. (1988b). Projections of nucleus angularis and nucleus laminaris to the lateral lemniscal nuclear complex of the barn owl. Journal of Comparative Neurology, 274, 212–238.

Tang, Y., Christensen-Dalsgaard, J., & Carr, C. E. (2012). Organization of the auditory brainstem in a lizard, Gekko gecko. I. Auditory nerve, cochlear nuclei, and superior olivary nuclei. Journal of Comparative Neurology, 520(8), 1784–1799.

ten Donkelaar, H. J., Bangma, G. C., Barbas-Henry, H. A., de Boer-van Huizen, R., & Wolters, J. G. (1987). The brain stem in a lizard, Varanus exanthematicus. Advances in Anatomy, Embryology, and Cell Biology, 107, 1–168.

Todd, N. P. M. (2007). Estimated source intensity and active space of the American alligator (*Alligator Mississippiensis*) vocal display. Journal of the Acoustical Society of America, 122(5), 2906.

Tollin, D. J. (2008). Encoding of interaural level differences for sound localization. In A. L. Basbaum, A. Kaneko, G. M. Shepherd, G. Westheimer, P. Dallos, & D. Oertel (Eds.), The senses: A comprehensive reference (Vol. 3, pp. 631–654). San Diego: Academic Press.

Urick RJ (1983) Principles of underwater sound (New York: McGraw-Hill).

van Dijk PP, Iverson J, Shaffer B, Bour R, Rhodin A (2011) Conservation Biology of Freshwater Turtles and Tortoises First. A. Rhodin, P. Pritchard, P. P. van Dijk, R. Saumure, K. Buhlmann, J. Iverson, and R. Mittermeier, eds. Chelonian Research Foundation.

Wagner, H. (2005). Microsecond precision of phase delay in the auditory system of the barn owl. Journal of Neurophysiology, 94(2), 1655–1658.

Wagner, H., Mazer, J. A., & von Campenhausen, M. (2002). Response properties of neurons in the core of the central nucleus of the inferior colliculus of the barn owl. European Journal of Neuroscience, 15(8), 1343–1352.

Wagner, H., Asadollahi, A., Bremen, P., Endler, F., Vonderschen, K., & von Campenhausen, M. (2007). Distribution of interaural time difference in the

barn owl's inferior colliculus in the low- and high-frequency ranges. Journal of Neuroscience, 27(15), 4191–4200.

Wagner, H., Brill, S., Kempter, R., & Carr, C. E. (2009). Auditory responses in the barn owl's nucleus laminaris to clicks: Impulse response and signal analysis of neurophonic potential. Journal of Neurophysiology, 102(2), 1227–1240.

Wang, Y., & Karten, H. J. (2010). Three subdivisions of the auditory midbrain in chicks (*Gallus gallus*) identified by their afferent and commissural projections. Journal of ComparativeNeurology, 518, 1199–1219.

Webb JF, Smith WL, Ketten DR (2006) The laterophysic connection and swim bladder of butterfly fishes in the genus Chaetodon (Perciformes: Chaetodontidae). J. Morphol. 267, 1338–1355.

Webb, J. F., Montgomery, J. C., & Mogdans, J. (2008). Bioacoustics and the lateral line system of fishes. In J. F. Webb, R. R. Fay, & A. N. Popper (Eds.), Fish bioacoustics(pp. 145–182). New York: Springer Science+Business Media.

Webster DB (1962) A function of the enlarged middle-ear cavities of the kangaroo rat, Dipodomys. Physiol Zool 35, 248–255

Weston, J. K. (1936). The reptilian vestibular and cerebellar gray with fiber connections. Journal of Comparative Neurology, 65, 93–199.

Wever, E. G. (1978). The reptile ear: Its structure and function. Princeton, NJ: Princeton University Press.

Wever, E. G., & Vernon, J. A. (1956a). Sound transmission in the turtle's ear. Proceedings of the National Academy of Sciences of the USA, 42(5), 292–299.

Wever, E. G., & Vernon, J. A. (1956b). Auditory responses in the common box turtle. Proceedings of the National Academy of Sciences of the USA, 42(12), 962–965.

Wever, E. G., & Vernon, J. A. (1956c). The sensitivity of the turtle's ear as shown by its electrical potentials. Proceedings of the National Academy of Sciences of the USA, 42(4), 213–220.

Wilczynski, W., & Capranica, R. R. (1984). The auditory system of anuran amphibians. Progress in Neurobiology, 22(1), 1–38.

Wild, J. M., Krützfeldt, N. O. E., & Kubke, M. F. (2010). Connections of the auditory brainstem in a songbird, Taeniopygia guttata. III. Projections of the superior olive and lateral lemniscal nuclei. Journal of Comparative Neurology, 518(11), 2149–2167.

Willis, K. L., McCormick, C. A., & Carr, C. E. (2011). The organization of the hindbrain auditory nuclei of turtles follows the sauropsid pattern. Neuroscience Meeting Planner. Washington,DC: Society for Neuroscience. Online. http://www.abstractsonline.com/Plan/ViewAbstract.

Willis, K. L., Christensen-Dalsgaard, J., Ketten, D. R., & Carr, C. E. (2013). Middle ear cavity morphology is consistent with an aquatic origin for testudines. (A. Iwaniuk, Ed.) Public Library of Science ONE, 8(1), e54086.

Willis, K. L., Christensen-Dalsgaard, J., & Carr, C. E. (2013b). Auditory Brain Stem Processing in Reptiles and Amphibians: Roles of Coupled Ears. In Springer Handbook of Auditory Research. New York, NY: Springer New York. doi:10.1007/2506_2013_24.

Winter, P., & Schwartzkopff, J. (1961). Form and cell number of the acoustic nerve center in the medulla oblongata of the owl (Striges). Experientia, 17, 515–516.

Witmer, L. M., & Ridgely, R. C. (2009). New insights into the brain, braincase, and ear region of tyrannosaurs (Dinosauria, Theropoda), with implications for sensory organization and behavior (P. Dodson, Ed.) The Anatomical Record: Advances in Integrative Anatomy and Evolutionary Biology, 292(9), 1266–1296.

Witmer, L. M., Ridgely, R. C., Dufeau, D. L., & Sermones, M. C. (2008). Using CT to peer into the past: 3D visualization of the brain and ear regions of birds, crocodiles, and non-avian dinosaurs. In H. Endo & R. Frey (Eds.), Anatomical imaging: Towards a new morphology (pp. 67–88). Tokyo: Springer-Verlag.

Wu, Y.-C., & Fettiplace, R. (1996). A developmental model for generating frequency maps in the reptilian and avian cochelas. Biophysical Journal, 70, 2557–2570.

Yan, K., Tang, Y.-Z., & Carr, C. E. (2010). Calcium-binding protein immunoreactivity characterizes the auditory system of Gekko gecko. Journal of Comparative Neurology, 518 (17), 3409–3426.

Young, B. (2003). Snake bioacoustics: Toward a richer understanding of the behavioral ecology of snakes. Quarterly Review of Biology, 78(3), 303–325.

Young, S. R., & Rubel, E. W. (1983). Frequency-specific projections of individual neurons in chick brainstem auditory nuceli. Journal of Neuroscience, 3(7), 1373–1378.

Zakon, H. H., & Wilczynski, W. (1988). The physiology of the anuran eighth nerve. In B. Fritzsch, M. J. Ryan, W. Wilczynski, T. Hetherington, & W. Walkowiak

(Eds.), The evolution of the amphibian auditory system (pp. 125–155). New York: John Wiley & Sons.

Zardoya, R., & Meyer, A. (2001). The evolutionary position of turtles revised. Naturwissenschaften, 88(5), 193–200.

Zeddies DG (2005) Development of the acoustically evoked behavioral response in zebrafish to pure tones. Journal of Experimental Biology 208, 1363–1372.